SUPPLEMENTARY INFORMATION

Sigma factor-mediated tuning of bacterial cell-free synthetic genetic oscillators

Maaruthy Yelleswarapu[+], Ardjan J. van der Linden[+], Bob van Sluijs, Pascal A. Pieters, Emilien Dubuc, Tom F.A. de Greef* and Wilhelm T. S. Huck[*]

Oscillator Model

An overview of the network can be found in Figure 1 of the main text. The corresponding ordinary differential equation (ODE) model uses Hill-type kinetics and can be found below. We explicitly model the binding of sigma-factors and RNA polymerase to account for competition and its effect on the network behavior. The other components of the model include descriptions of transcription and translation of the activator gene construct **P_{70}-σ_{28}** (DNA_Y/$DNA_{Activator}$), repressor gene construct **P_{28}-C1-ssra** (DNA_Z/$DNA_{Repressor}$), and reporter gene construct **P_{70}-deGFP** (DNA_X/$DNA_{Reporter}$).

RNA Polymerase

$$\dot{RNAP} = -(\deg_{pol} + dil) * RNAP + RNAP_0 * dil - kf_{RS70} * RNAP * S70 + kr_{S70} * RS70 - kf_{RS28} * S28 * RNAP + kr_{RS28} * RS28 \quad 1.1$$

$$\dot{RS70} = -(\deg_{pol} + dil) * RS70 + kf_{RS70} * RNAP * S70 - kr_{S70} * RS70 \quad 1.2$$

$$\dot{RS28} = -(\deg_{pol} + dil) * RS28 + kf_{RS28} * RNAP * S28 - kr_{S28} * RS28 \quad 1.3$$

$$\dot{S70} = -(deg_{S70} + dil) * S70 + S70_0 * dil - kf_{RS70} * RNAP * S70 + kr_{RS70} * RS70 \quad 1.4$$

P_{70}-σ_{28} Construct

$$\dot{mRNA}_{S28} = -(deg_{mRNA} + dil) * mRNA_{S28} + DNA_{Activator} * vmax_{RS70} * \frac{\frac{RS70}{kd_{RS70}}}{1 + \frac{RS70}{kd_{RS70}} + \left(\frac{C1}{kd_{c1}}\right)^{Nci}} \quad 1.5$$

$$\dot{S28} = -(deg_{S28} + dil) * S28 + ktrans_{S28} * mRNA_{S28} - kf_{RS28} * RNAP * S28 + kr_{RS28} * RS28 \quad 1.6$$

P_{28}-C1-ssra Construct

$$\dot{mRNA}_{C1} = -(deg_{mRNA} + dil) * mRNA_{C1} + DNA_{Repressor} * vmax_{RS28} * \frac{\left(\frac{RS28}{kd_{RS28}}\right)^{N28}}{1 + \left(\frac{RS28}{kd_{RS28}}\right)^{N28}} \quad 1.7$$

$$\dot{C1} = -(deg_{C1} + dil) * C1 + ktrans_{C1} * mRNA_{C1} \quad 1.8$$

P_{70}-deGFP Construct

$$(\dot{mRNA}_{deGFP}) = -(deg_{mRNA} + dil) * mRNA_{deGFP} + DNA_{Reporter} * vmax_{RS70} * \frac{\frac{RS70}{kd_{RS70}}}{1 + \frac{RS70}{kd_{RS70}} + \left(\frac{C1}{kd_{c1}}\right)^{Nci}} \quad 1.9$$

$$\dot{eGFP}_{dark} = -(k_{mat} + deg_{deGFP} + dil) * deGFP_{dark} + ktrans_{deGFP} * mRNA_{deGFP} \quad 1.10$$

$$\dot{eGFP} = -(deg_{deGFP} + dil) * deGFP + k_{mat} * deGFP_{dark} \quad 1.11$$

Equations 1.1 to 1.4 model the RNA polymerase, sigma factors and their respective holoenzymes, using general mass action kinetics where kf and kr are the respective forward

and reverse binding rates[1]. The $RNAP_0$ and $S70_0$ are constants representing static concentrations flowing into the reactor scaled by the dilution rate (these are simultaneously the initial conditions of RNAP and σ_{70} in each simulation). Equations 1.5-1.6 model the transcription and translation of σ_{28} gene, using hill type kinetics for the regulation of the transcription[2]. Equations 1.7-1.8 model the *C1* gene, and equations 1.9-1.11 the *deGFP* gene. We do not have a hill coefficient included for regulation of genes by σ_{70}. Basal gene transcription resembles Michealis Menten kinetics[1,3], when estimated using experimental data its value was around 1, therefore excluded it from the model. The translation process is modeled with a mass action term. Finally, the parameters of **P_{70}-σ_{28}** template, **P_{28}-C1-ssra** template, **P_{70}-deGFP** template and the **Refresh Rate** (*dil*) are the experimentally controlled parameters and make up the control space. Henceforth we will refer to these parameters as the control parameters and the remainder as the model parameters. Prior to estimating the model parameters and predicting experimental outcomes for combinations of control parameters we explored the effect of the model parameters on our desired behavior – oscillations in flow TX-TL conditions.

(Note: In the main text we refer to experiments in the microfluidic device as steady-state TX-TL conditions. However, since we will use similar terminology in this appendix , we will refer to steady-state TX-TL experiments as flow TX-TL experiments.)

Latin Hypercube Sampling and Analysis

Novak and Tyson described that for a system to oscillate, a time-delay, sufficient non-linearity, a feedback loop and balanced rates are needed[4]. To test if this motif could oscillate in flow TX-TL conditions and to explore the subsequent relationship between parameters, the amplitude and periodicities, we sampled the parameter space for our model using Latin hypercube sampling (LHS)[5]. The upper and lower boundaries for each sample were based on previously published work[3,6] (Table S1). We ran the simulations until steady-state conditions

were reached. We found that 29% of the sampled parameter sets have a stable limit cycle, indicating that the motif is robust in its ability to produce oscillations (Figure S1a). We show the distribution of amplitudes and periodicities as an indicator of the expected behaviour, noting a median amplitude 13 nM (Figure S1b) and a median periodicity of 140 minutes (Figure S1c), indicating that long periods and low amplitude oscillations are common within the sampled space.

We show the Pearson correlation coefficient for each parameter and the amplitude (Figure S1d) and periodicity to test for correlation and outline two observations (Figure S1e). Firstly, increased **Refresh Rate** and degradation rates correlate with lower amplitudes whereas higher transcription, translation rates and concentrations of the **P_{70}-deGFP** template correlate with higher amplitudes. Second, there exists a negative correlation between amplitude and the following parameters: the dissociation constant (kd_70), concentration of **P_{70}-σ_{28}** template, the forward binding rate (kf_RS28) of σ_{28} (its competitive strength) and the transcription rate of σ_{28} . A positive correlation exists between amplitude and the dissociation constant (kd_28) ,the reverse binding rate (kr_RS28) of σ_{28} to the RNAP. This indicates that a strong activator shortens the time delay needed between the initial activation and the feedback response by the C1 protein. For periodicity the **Refresh Rate** and degradation are the key factors. An increase in the dilution of the system shortens the periodicity of the system, and an increase in the Hill coefficients increases the periodicity, indicating that stepwise response for both the activation and feedback lengthens the period of the oscillation.

Next, we explored the relationship between the parameters and the probability of a limit cycle by performing a logistic regression with oscillations (1) or no oscillations (0) as response variable and the individual parameters as predictors. We subsequently exponentiated the resulting parameter estimation to obtain the odds ratio, a metric which indicates the probability of a limit cycle moving a single unit (minimum to maximum parameter value)

along the axis of the predictor (Figure S1f). Note that this is a crude estimate and is best used to study the relative differences between the parameters itself, but it underscores the previous assertion regarding the strength of the activation, high values for parameters driving the activation of the feedback response have lower odds of resulting in a stable limit cycle.

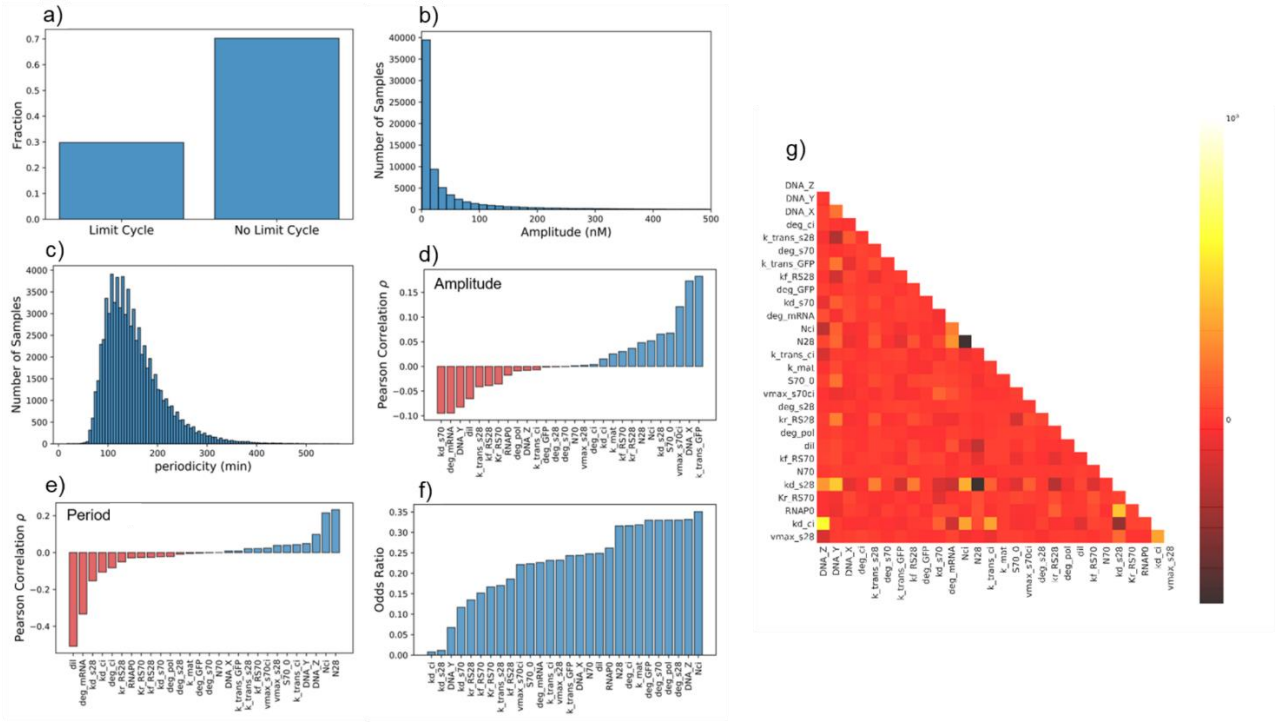

Figure S1 Result of the latin hypercube sampling. 250,000 parameter sets were sampled between the boundaries shown in Table S1, the distributions illustrate the space in which the network operates, the statistical analysis highlights potential drivers of behaviour. **(a)** A fraction of parameter sets with a stable limit cycle (29%) and without (71%). **(b)-(c)** distribution of the amplitudes and periodicities found in the subset of parameters which have a stable limit cycle (for **(b)** we limit the x-axis to 500 nM, though higher values were observed for large reporter gene concentrations they were very infrequent). **(d)-(e)** Pearson correlation between the parameters and the amplitude and periodicity respectively, a negative correlation is indicative of a lower amplitude or periodicity for a higher parameter value. **(f)** The odds resulting from a logistic regression with the presence of a limit cycle (1 or 0) and the parameters. This analysis is only suited as a relative comparison between parameters. **(g)** Pearson correlation between model parameters within sample subset with a stable limit cycle. The colour in the squares indicate the type of correlation, positive (white) , negative (black), and neutral (red). The colour bar was scaled by taking the symlog of the coefficients.

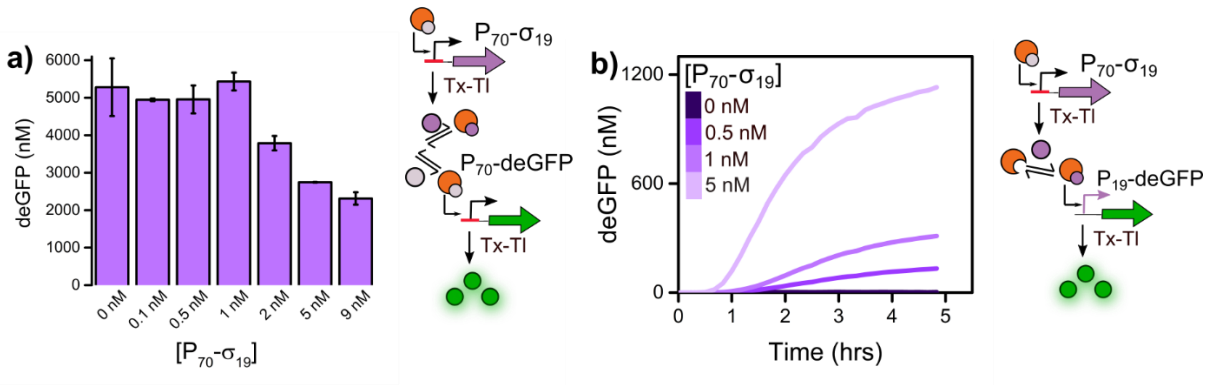

Figure S2 Time traces of deGFP production as readout for the key regulatory mechanisms of the σ_{19}-oscillator under batch TX-TL conditions **(a)** End-point expression of deGFP from **P_{70}-deGFP** under competition for core RNAP between sigma factors σ_{70} and σ_{19}. Increasing concentrations of **P_{70}-σ_{19}** template were added to 5 nM of **P_{70}-deGFP**. We observed that 5 nM of **P_{70}-σ_{19}** is required to produce enough σ_{19} to outcompete σ_{70} for the core RNAP and reduce deGFP expression from **P_{70}-deGFP** template by approximately 50%, as compared to 0.5 nM of the **P_{70}-σ_{28}** template (Figure 2c). **(b)** Two-step σ_{19}-activation cascade. Increasing concentrations of **P_{70}-σ_{19}** template were added to 5 nM of **P_{19}-deGFP** template. Increased deGFP production from **P_{19}-deGFP** with increasing **P_{70}-σ_{19}** template concentrations was observed, however the fold change in protein production between 0.5 nM and 5 nM of **P_{70}-σ_{19}** template was much larger as compared to σ_{28} (Fig 2c).

Evolutionary Algorithm Overview and Operations

Figure S3 gives an overview of the Evolutionary algorithm. This algorithm was created in python 2.7 (Python Software Foundation, www.python.org). The source code can be found on github https://gitlab.com/huckgroup. All simulations were solved using the scripy integrate package and the LSODA solver. The EA itself uses element form previously published work[7], specifically some of the EA operations. The user supplies a text file with model information including the differential equations, states, (control) parameter boundaries, and a csv file with the experimental data for parameter estimation. The EA parses these files and builds a model including a parameter space. Two initial parental networks are recombined to produce offspring ψ_i. This offspring is mutated, solved and scored. This cycle is repeated 10 times , the 2 fittest networks are chosen, and the steps are repeated. We

maintained a maximum number of generations as a termination criterion (2000). We detail the steps below.

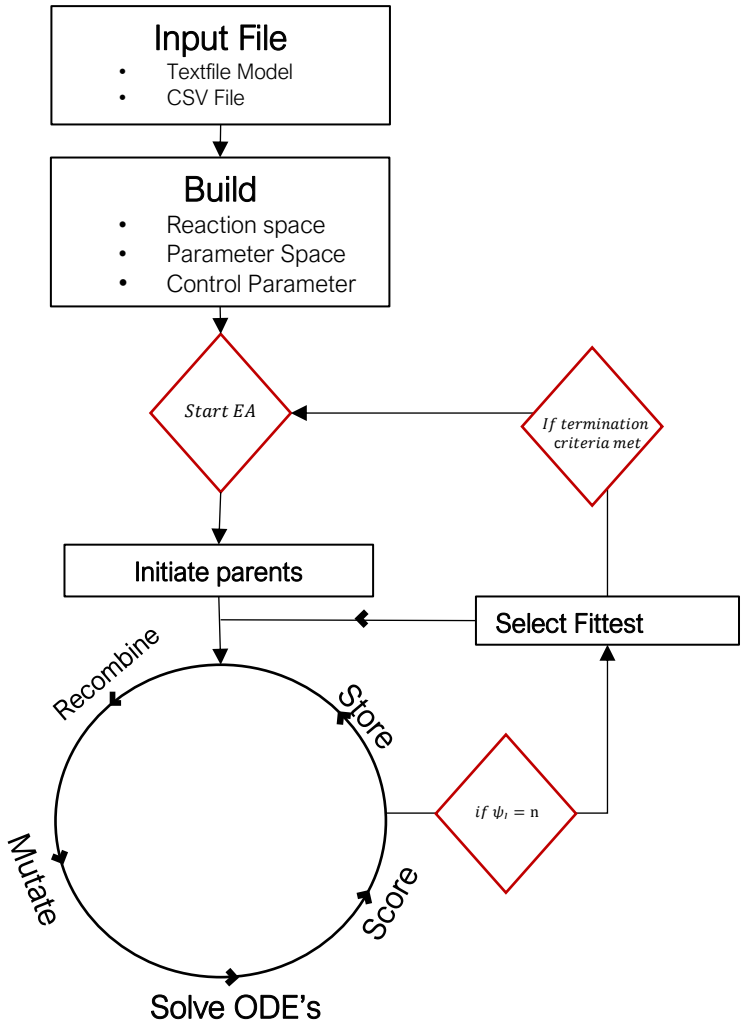

Figure S3 A schematic overview[8] of the EA used to fit experimental data to estimated model parameters. Initial parental parameter sets are recombined, mutated, solved and scored, this is repeated ten times and marks a single generation. From this generations the two fittest parameter sets are selected to re-enter the cycle again. This is done until a termination criterion is met (maximum number of generations in our case).

Building

The parameter space for a single parameter is created by building a (uniform) logarithmically spaced vector V with n the size of the vector (100). The individual parameters $V_i = 10^{\theta_i}$ where θ_i is sampled from a uniformly distributed vector θ defined by $\theta = \left\{\text{r: } \exists \text{i } \epsilon \mathbb{N} \text{ such that r} = log_{10}(\alpha) + \frac{log_{10}(\beta)}{\text{n}} i, \text{and r } \epsilon \left[log_{10}(\alpha), log_{10}(\beta)\right)\right\}$ where α and β are the respective upper and lower boundary of a parameter as defined by the user. For the boundaries α and β see Table S1.

Recombination

Two parental parameters sets are created and recombined, the EA loops through the model parameters to build a new parameter vector ζ selecting a new value for parameter j with probability p from the two parental parameter sets $\gamma$and ε according to $(\forall p < 0.5 \rightarrow \zeta_j = \gamma_j) \wedge \left(\forall p \geq 0.5 \rightarrow \zeta_j = \varepsilon_j\right)$

Mutation

This offspring is subsequently mutated by randomly sampling a new value from ζ or by moving one position ζ_{i+1} or ζ_{i-1} within this vector given an initial value with a corresponding vector index. The probability for either action is equal.

Scoring

The output of the network -*deGFP*- is subsequently scored. We use two scoring functions to fit the data, calculating the score for a number of experimental time-series M (i.e. different experimental conditions).

$$\partial_1 = \sum_{i=1}^{m} \sum_{j=1}^{t_p} (d_j^i - y_j^i)^2$$

$$\partial_2 = \sum_{i=1}^{m} \sum_{j=2}^{t_p} (\frac{d_j^i}{\Delta t} - \frac{\Delta y_j^i}{\Delta t})^2$$

Where ∂_1 is the residual squared error between the simulated time-series data with and the experimental data set, t_p the simulated time-points. ∂_2 the same but for rates of change, where $\Delta x/\Delta t$ changes in $x(\Delta x_j^i = x_j^i - x_{j-1}^i)$ per time step Δt.

Selection

If the user defined – maximum offspring number per generation n – is reached, the EA selects the fittest parents and restarts the cycle. We maintain rank based selection with multiple objectives for both the parameter fit to qualitatively distinguish between improvements in either score. Thus, the comparison between the desired system function and simulations yields a vector of objective scores, $\vec{\Delta} = \{\partial 1, \partial 2, \ldots, \partial n\}$. The EA ranks these scores individually, sums them and selects the parameter set with the lowest rank. So, given a set of *N* objective scores for *M* sets, we calculate the rank matrix $\boldsymbol{\Xi}$ based on the scores in Δ:

$$\Xi = \begin{bmatrix} \xi_{1,1} & \cdots & \xi_{N,1} \\ \vdots & \ddots & \vdots \\ \xi_{1,M} & \cdots & \xi_{N,M} \end{bmatrix}$$

$\vec{\Xi} = (\| \xi_{1*} \|, \| \xi_{2*} \|, \ldots, \| \xi_{N*} \|)$ representing the L_n-norm of each column. The optimal network is then obtained from min($\vec{\Xi}$).

Estimating Model Parameters and Control Space Exploration.

We used the EA to estimate the parameters 150-250 times for each of the batch TX-TL experiments (Figure 2). Each batch TX-TL experiment was set up to identify different model parameters. We tested different concentration of the **P_{70}-deGFP** template (Fig 2a) to get an estimate of the following system parameters: $ktrans_{deGFP}, vmax_{RS70}, deg_{deGFP},$. The σ_{28}-activation cascade dataset (Figure 2b) was used to estimate parameters related to of transcription by σ_{28}, including: $vmax_{RS28}, ktrans_{S28}$. The competition dataset (Figure 2c)

was used to identify the binding rates for σ_{28} and σ_{70} sigma factors to the RNA polymerase, including: kf_{RS70}, kr_{RS70} , kf_{RS28} , kr_{RS28}, $RNAP_0$, $S70_0$. The repression by C1 dataset (Figure 2d) was used to estimate all the system parameters involving the repressor protein C1, including: $Nci, kd_{c1}, vmax_{RS70}, ktrans_{C1}, deg_{C1}, deg_{mRNA}$. Figure S4 shows the results of the fits and the parameter values can be found in Table S1 and can be considered an initial estimate, it is likely that the estimated parameters are a function of the experimentally controlled DNA concentrations and could vary on implementing the network into a different environment (from batch TX-TL to flow TX-TL) for example, it is reasonable to assume that increases in the total concentration of DNA modifies transcription and translation rates across the board as cellular resources are redistributed.

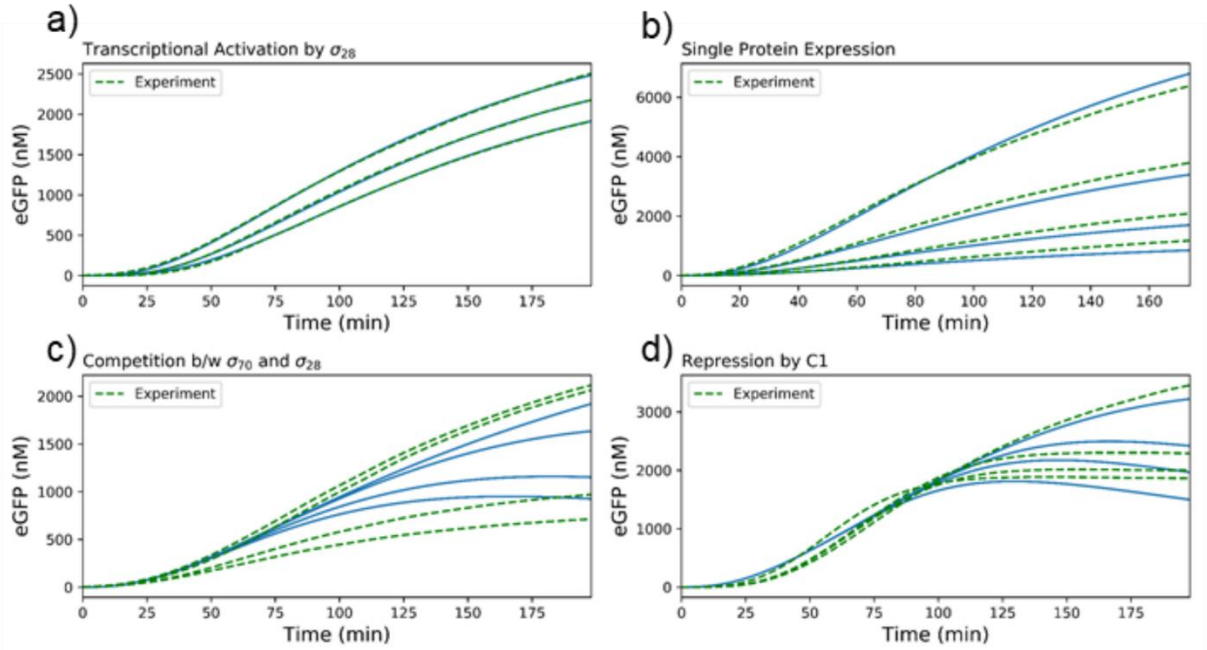

Figure S4 An overview of the different parameter estimations by the EA. The batch TX-TL experiments were fitted separately **(a)** σ_{28}-transcriptional activation cascade (Figure 2b) **(b)** **P_{70}-deGFP** concentration range batch TX-TL (Figure 2a) **(c)** Expression from **P_{70}-deGFP** under competition for core RNAP between sigma factors σ_{70} and σ_{28} (Figure 2c) **(d)** Transcriptional repression by C1 (Figure 2d). The green lines are the experimental data, the blue lines the fits. The number of fits per batch experiment ranges between 150-250. (Note: we attempted to fit all the experimental data simultaneously, however the EA would not converge, hence we show the best fits).

We used the system parameter set (Table S1) to explore the control parameter space **P_{70}-σ_{28}** template, **P_{28}-C1-ssra** template, **P_{70}-deGFP** template and the **Refresh Rate**. We fixed the concentration of the **P_{70}-deGFP** reporter template at 8 nM and tested a combination of 25 uniformly spaced points for each of the other control parameters to search for stable oscillations (limit cycles). We estimated the subset of the control parameter space for which the model predicts stable oscillations with an amplitude greater than 20 nM in deGFP expression (Figure S5a). This cutoff is used to ensure we can observe oscillations experimentally. Figure S5a shows the region of the control space where a stable limit cycle was found. We found that the network maintains a stable limit cycle over a broad range of **P_{28}-C1-ssra** template concentrations and **Refresh Rates**. However, the limit cycle disappears as the concentration of the **P_{70}-σ_{28}** template increases, a result in agreement with the LHS analysis (Figure S1d-e). Figure S5b is a slice of the control parameter space shown in Figure S5a, where we plot the amplitude as a function of the **P_{70}-σ_{28}** template and **P_{28}-C1-ssra** template concentration. We observe a decrease in amplitude as the concentration of **P_{70}-σ_{28}** template increases, an effect partially compensated for by low concentrations of **P_{28}-C1-ssra** template and high refresh rates. Finally, Figure S5c shows the density of the amplitudes and periodicities found in the oscillating space, with low amplitude oscillations dominating the space.

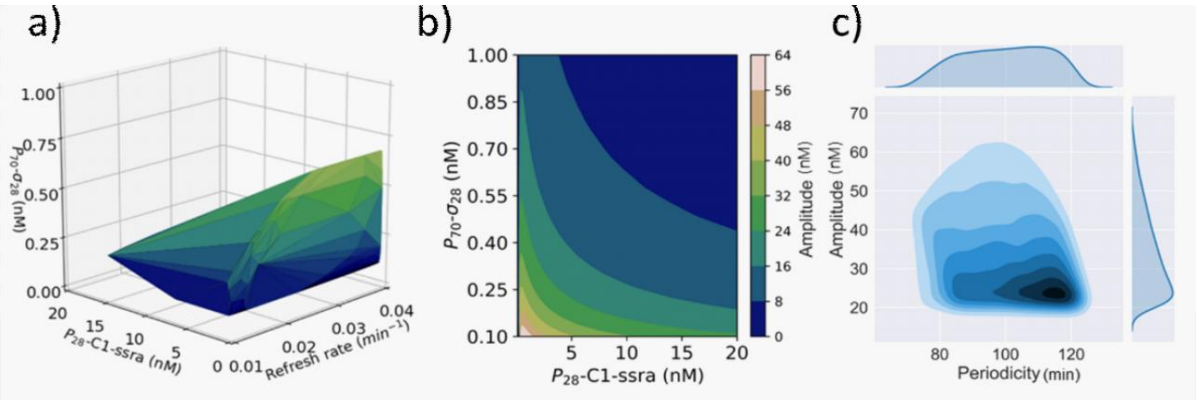

Figure S5 (a) The oscillating regime in the control parameter space, the space is approximated by a combination of 25 uniformly sampled points for each control parameter for the σ_{28}-oscillator. We used a convex hull algorithm to find the outer points of the scatter cloud and connected them using a Delauney algorithm (from the scipy and matplotlib library respectively), we remove limit cycles with an amplitude of less than 20 nM from the scatter cloud to ensure we can observe the limit cycle experimentally, the colour variation corresponds to the z-axis (activator). **(b)** A slice of the control space shown in **(a),** taken along the refresh rate axis at a value of 0.026 min^{-1}, the colorbar indicates the amplitude of the oscillations at steady state in nM. **(c)** The observed amplitudes and periodicities found in the oscillating space are broken down in a probability density plot.

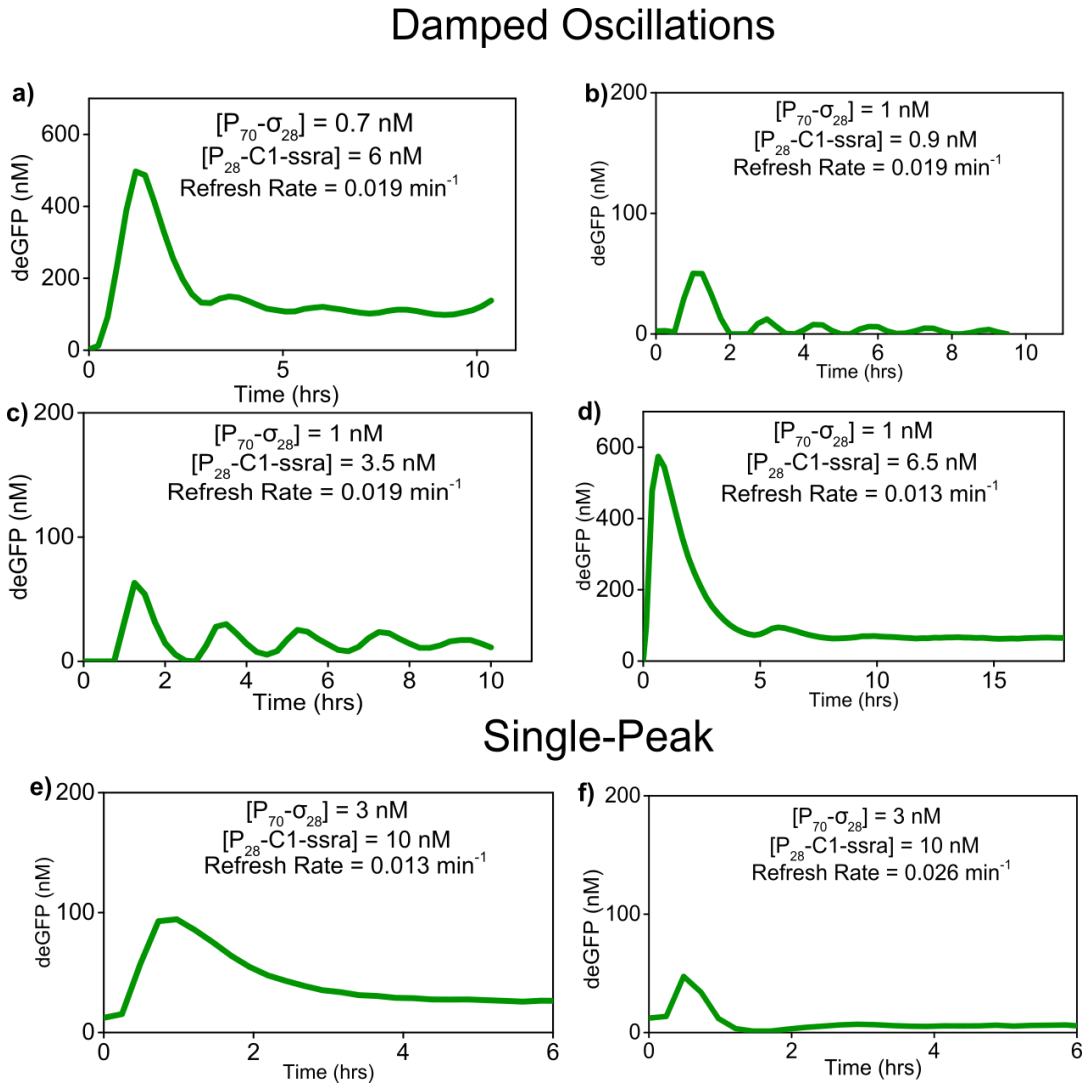

Figure S6 Experimentally obtained deGFP traces exemplifying the damped oscillations and single-peak behaviour of the σ_{28}-oscillator under steady-state TX-TL conditions. **P_{70}-deGFP** DNA template concentration

was fixed at 8 nM in all experiments. The concentrations of **P_{70}-σ_{28}**, **P_{28}-C1-ssra** templates and the **Refresh Rate** values for each experiment are as indicated.

We re-estimated the parameters with the flow TX-TL data and found limit cycles exist for higher concentrations of **P_{70}-σ_{28}** than previously predicted. To capture the transition from a stable steady state to a limit cycle, we used an experimental point within and outside the oscillating regime to fit the model to the data and update our parameter values (Figure S7). Upon doing so we found that there no single parameter set which can uniquely describe the system. We show the distribution of amplitude and periods for the top 25 parameter sets (Figure S7 b and c) out of which we chose the parameters which show the best fit (Figure S7 d and e). The updated parameter values can be found in Table S1.

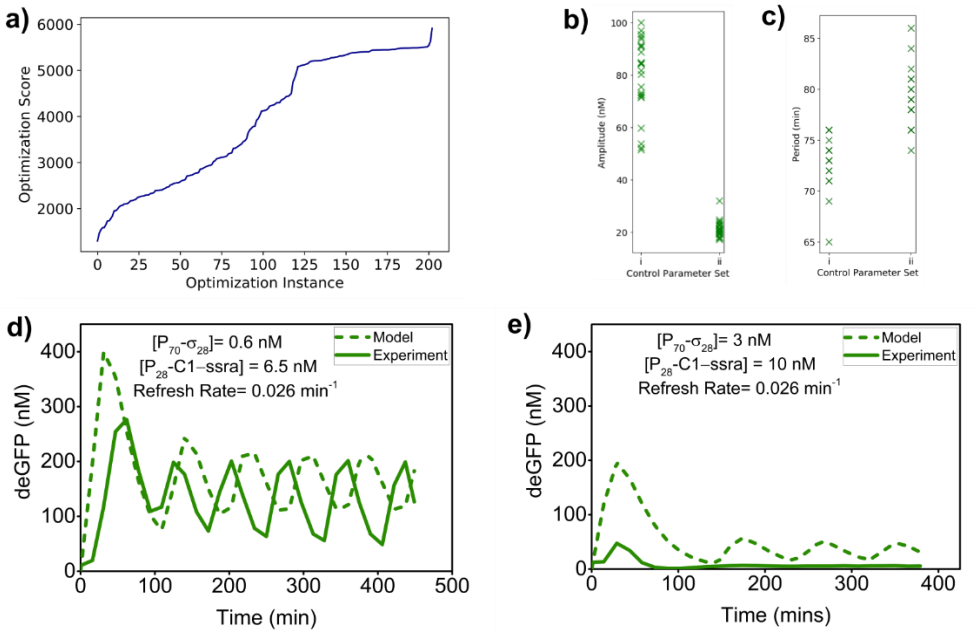

Figure S7 **(a)** Sorted convergence scores for 200 model parameter estimation instances (lower score indicates better fit to the data). **(b)** Amplitudes and **(c)** periods for the the top 25 (with best convergence score) optimised model parameter sets from **(a)** for two control parameter sets. The values of the control parameters in (i) are **P_{70}-σ_{28}** = 0.6 nM, **P_{28}-C1-ssra** = 6.5 nM, **Refresh Rate** = 0.026 min^{-1} **, P_{70}-deGFP =** 8 nM and for (ii) are **P_{70}-σ_{28}** = 3 nM, **P_{28}-C1-ssra** = 10 nM, **Refresh Rate** = 0.026 min^{-1} **, P_{70}-deGFP =** 8 nM **. (d)** and **(e)** Model-simulated and experimentally-obtained time traces for the parameter set showing the best fits. The traces are simulated

from the parameters obtained by fitting the model to steady-state data as shown in Table 1. We chose a data point inside (d) (Figure 3a(iii)) and outside (e) the oscillating regime to improve our parameter estimation.

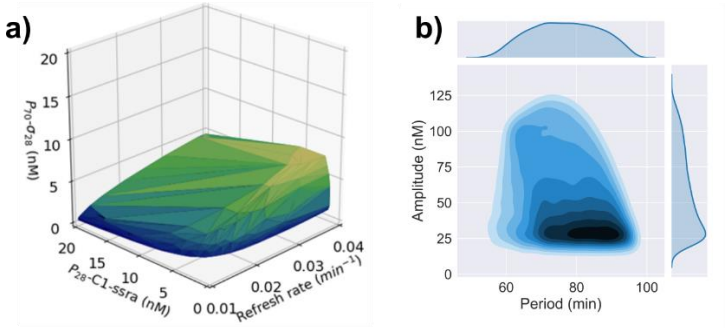

Figure S8 **(a)** Model-predicted oscillating subset of the control parameter space of the σ_{28}-oscillator. Colours on the plot correspond to the [$\mathbf{P_{70}\text{-}\sigma_{28}}$] axis **(b)** Probability density plot of the amplitudes and periods of oscillations within this subset.

Sensitivity Analysis

We performed two sequential sensitivity analyses: we assessed the impact of changing a single system parameter on the periodicity and amplitude of the oscillations. We use this analysis as a guide and explored the effect of changing system parameters on the size of the oscillating region in the control space. For the first analysis we fixed the control parameters to be the centroid ($\mathbf{P_{70}\text{-}\sigma_{28}}$ =1.16 (nM), $\mathbf{P_{28}}$**-C1-ssra** = 7.55 (nM), **Refresh Rate** = 0.021 min^{-1}) of the oscillating region (Figure S8a), to reduce distortions caused by boundary values. Figure S9 shows the initial sensitivity analysis. Since increased concentrations of $\mathbf{P_{70}\text{-}\sigma_{28}}$ reduce the amplitude of oscillations and dampens the system we assume that the required modification should increase the amplitudes. The results posit three such modifications; increasing competitive strength or concentration of σ_{70}, increasing the dissociation constant of the C1 repressor, or decreasing the competitive strength of σ_{28}. Figure S10 confirms that the overall size of the oscillating region increases by reducing the strength of the sigma factor, which rules out unforeseen (negative) effects from other control parameters on the size of the oscillating region after modification.

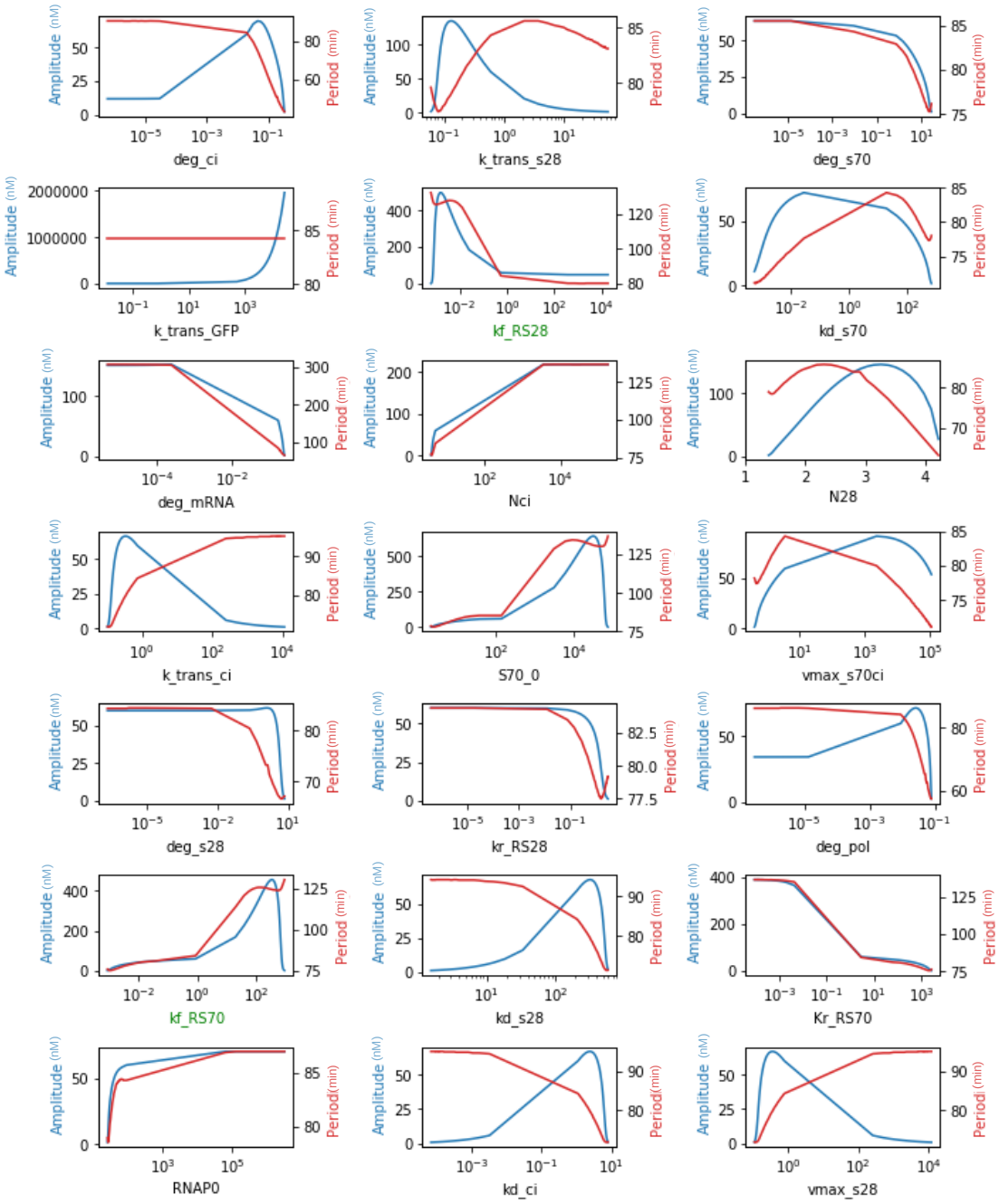

Figure S9. Sensitivity analysis of individual parameters, exploring the effect of parameter perturbations of the amplitude and periodicity of the network. It shows that the amplitude of the deGFP oscillations increases by decreasing the rates associated with the activator. The forward binding rates (green) of σ_{28} and σ_{70} have significant (mirrored) effect on the amplitude and can be considered targets for modification.

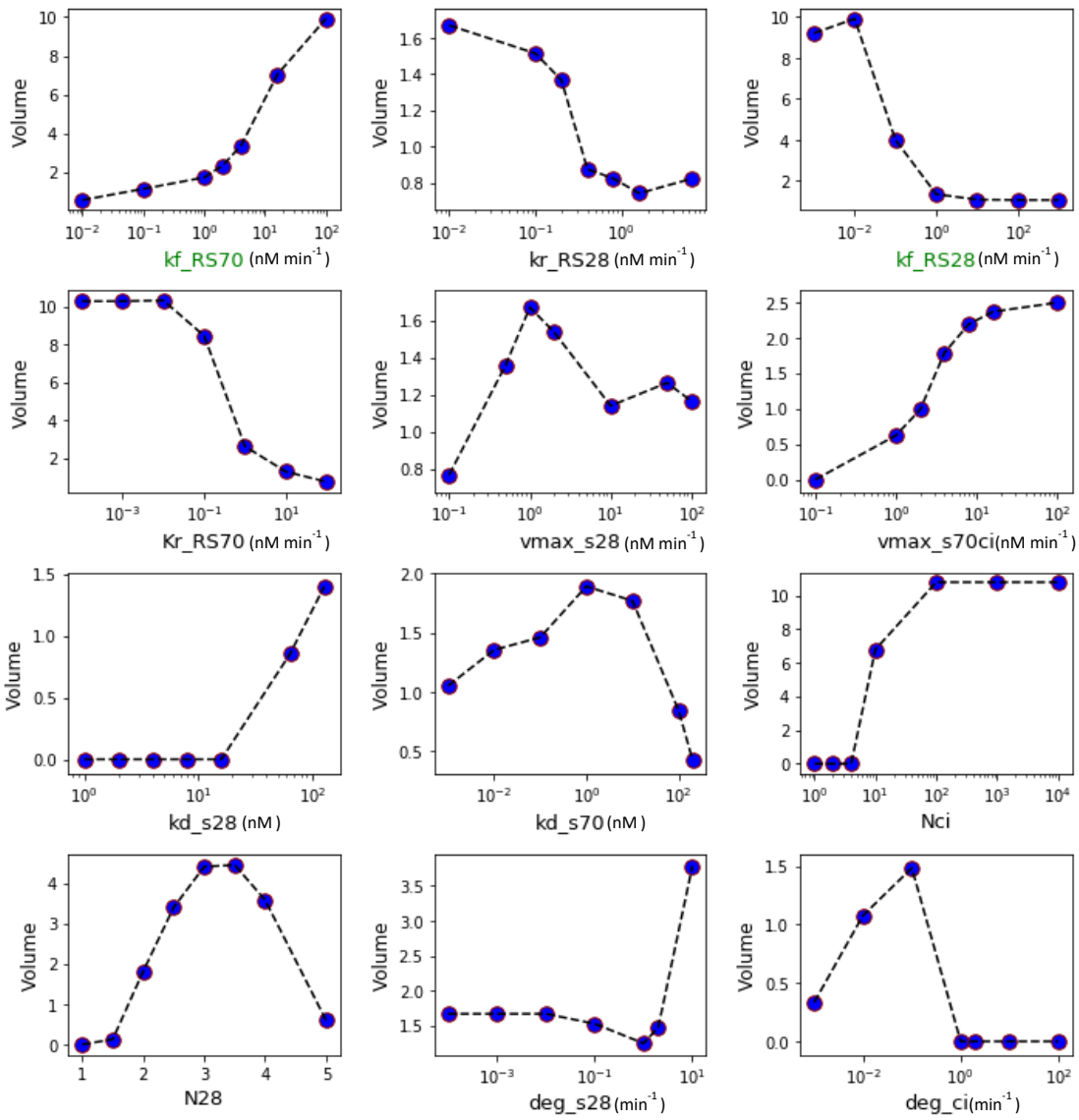

Figure S10 Sensitivity analysis of individual parameters exploring the effect of parameter perturbations. It confirms the negative effect of σ_{28}. 7 values for each parameter were tested, the ranges were set manually based on the effect of parameter perturbations on oscillation amplitudes. The correlation between an increase in amplitude and the size of the oscillating region holds true for the decrease in competitive strength of the activating sigma factor. The volume (y-axis) corresponds to the size of the oscillating region across three dimensions shown in Figure S5a. The volume is a function of the concentration of the **P_{70}-σ_{28}** (nM) and **P_{28}-C1-ssra** (nM) template concentration and **Refresh Rate** (min^{-1}).

We characterized the control parameters space for the σ_{19}-oscillator, assuming Kf_S19 to be six times lower than Kf_S28 and vmax_s19 was set to half that of vmax_s28 (based on

literature values and batch experiments in Figure S2) and set Kf_S70 to be four times higher (increased activity was observed because of the different batch of TX-TL reaction mixture)[9]. Figure S11a shows the composition highlighting the improvement in obtaining robust oscillations by modifying only a single component in the network.

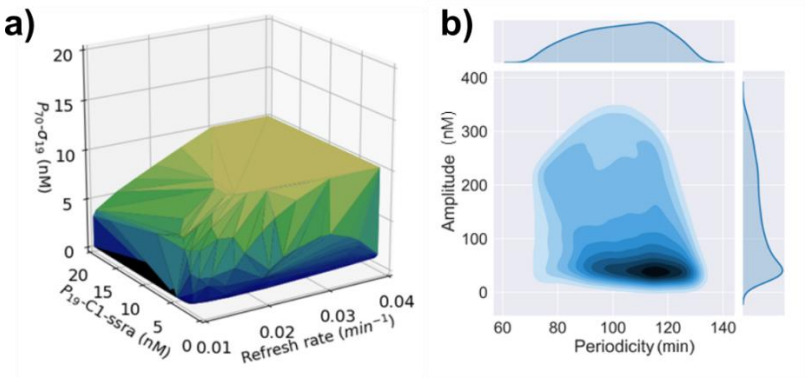

Figure S11 **(a)** Model-predicted oscillating subset of the control parameter space of the σ_{19}-oscillator. Colours correspond to the [**P_{70}-σ_{19}**] axis **(b)** Probability density plot of the amplitudes and periods of oscillations within the oscillating subset.

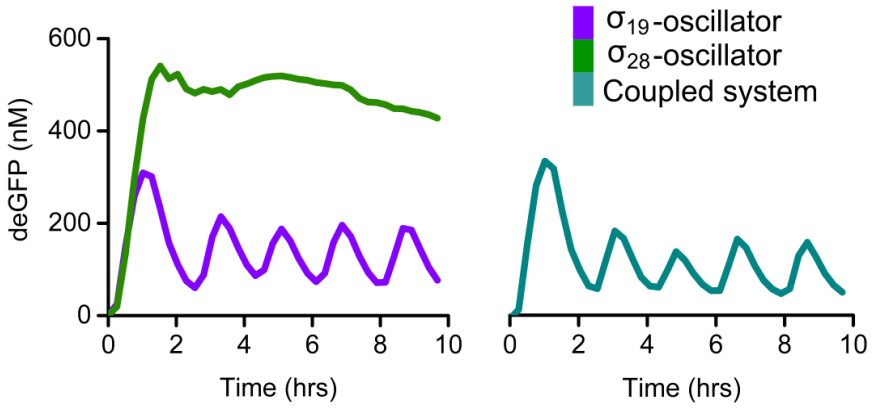

Figure S12 deGFP traces of the σ_{28}-oscillator, σ_{19}-oscillator and the coupled system under steady-state TX-TL conditions. The concentration of **P_{70}-deGFP**, **P_{19}-C1-ssra**, **P_{70}-σ_{19}** ,**P_{70}-σ_{28}** and **P_{28}-C1-ssra** were 8 nM, 6.5 nM, 10 nM, 0.4 nM and 0.9 nM respectively.

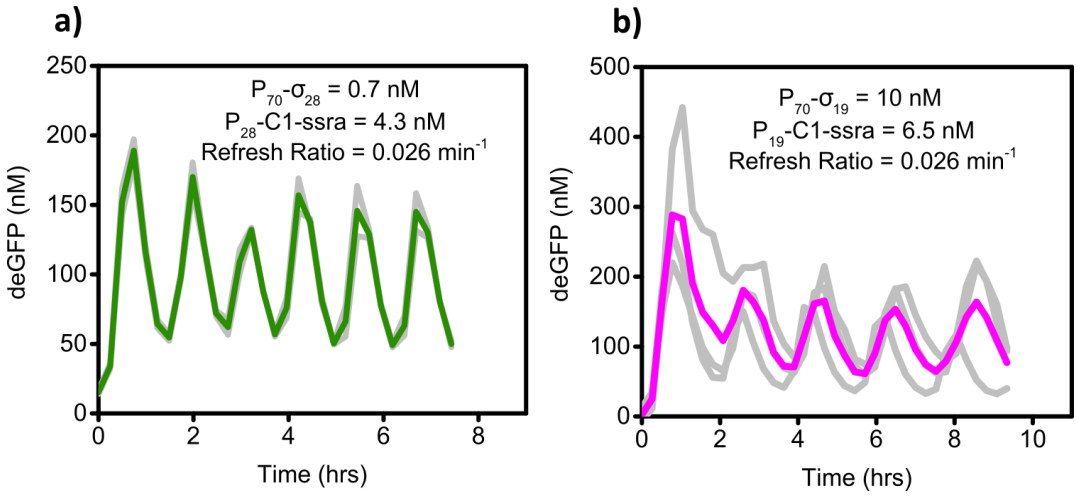

Figure S13 Oscillation experiments **(a)** in two independent reactors in a single microfluidic chip (gray lines are the individual reactors and green is the average) **(b)** across three different microfluidic chips (gray lines are oscillations from individual chips and violet is the average). **P_{70}-deGFP** template concentration was fixed at 8 nM in both cases.

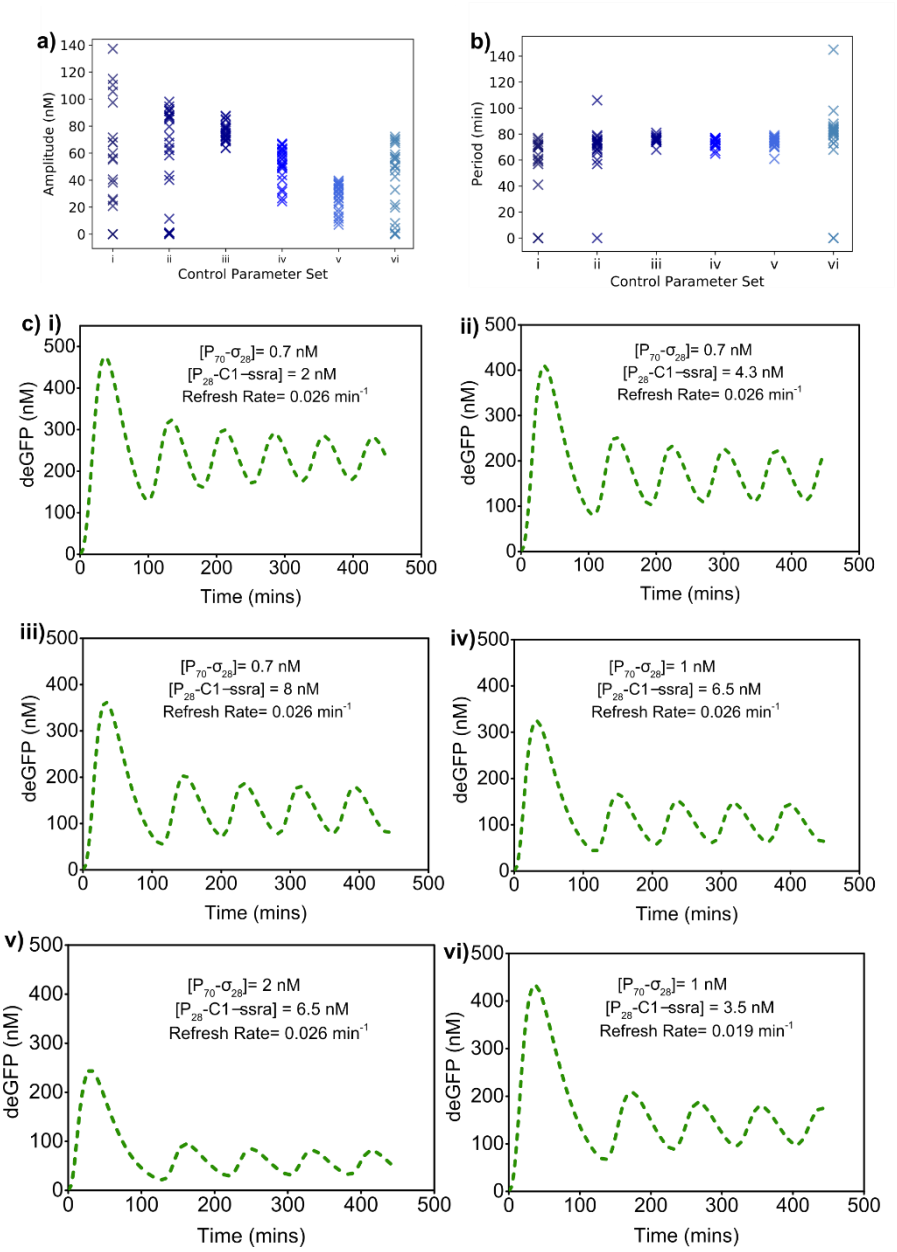

Figure S14 **(a)** Amplitudes and **(b)** Periods obtained by simulating the top 25 (with best convergence score) optimised model parameter sets from S7(a) for the different control parameter sets (i)-(vi) of the σ_{28}-oscillator. **(c) (i)-(vi)** Model-simulated time traces for the σ_{28}-oscillator . The traces are simulated from the parameters in Table 1. **P_{70}-deGFP** concentration was 8 nM. The values of the control parameters for the control parameter sets in **(a)** and **(b)** i-vi correspond to the values shown in **(c) (i)-(vi)**.

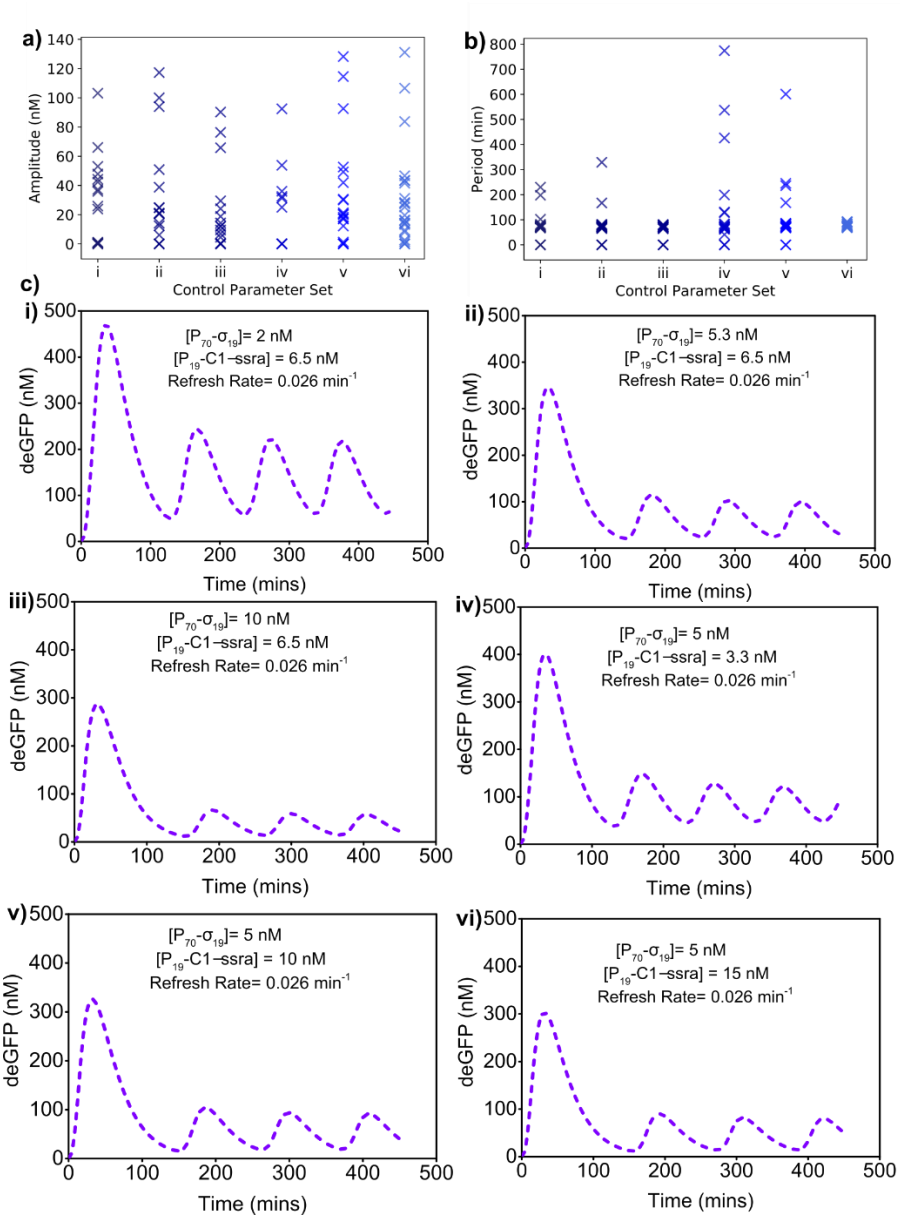

Figure S15(a) Amplitudes and **(b)** Periods obtained by simulating the top 25 (with best convergence score) optimised model parameter sets from for the different control parameter sets i-vi of the σ_{19}-oscillator. **(c) (i)-(vi)** Model-simulated time traces for the σ_{19}-oscillator. The traces are simulated from the parameters in Table 1.The values of the control parameters for the control parameter sets in **(a)** and **(b)** i-vi correspond to the values shown in **(c) (i)-(vi)**.

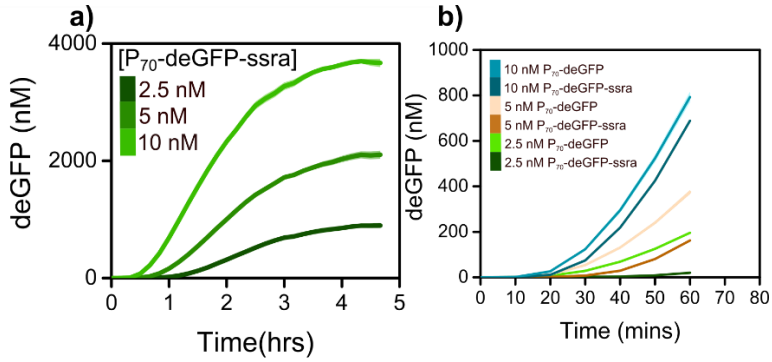

Figure S16 (a) Batch TX-TL reaction of **P_{70}-deGFP-ssra** template concentration range. The ssra tag on the C terminus of a protein targets the protein for additional degradation by the ClpXP proteases in the lysate. Shaded error bands are standard error of three separate measurements. **(b)** Comparison of the initial rates of production of ssra tagged and untagged deGFP protein from **(a)** and Figure 2a. We found no significant difference in end-point yield of tagged and untagged deGFP. However, ssra-tagged deGFP was produced at a lower rate as compared to the untagged version.

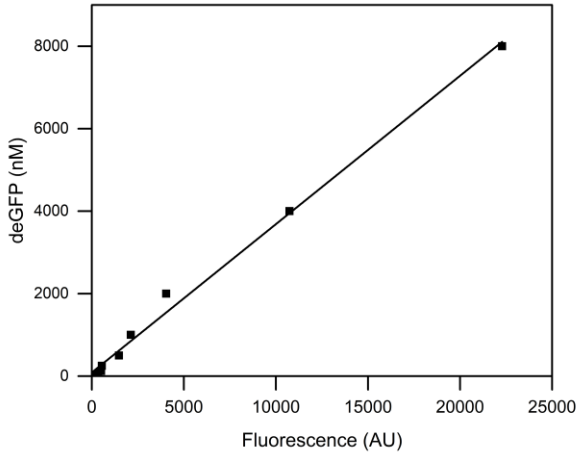

Figure S17 Fluorescence of different concentrations of purified protein were measured to calibrate the deGFP fluorescence.

Fabrication and Operation of Microfluidic Chip

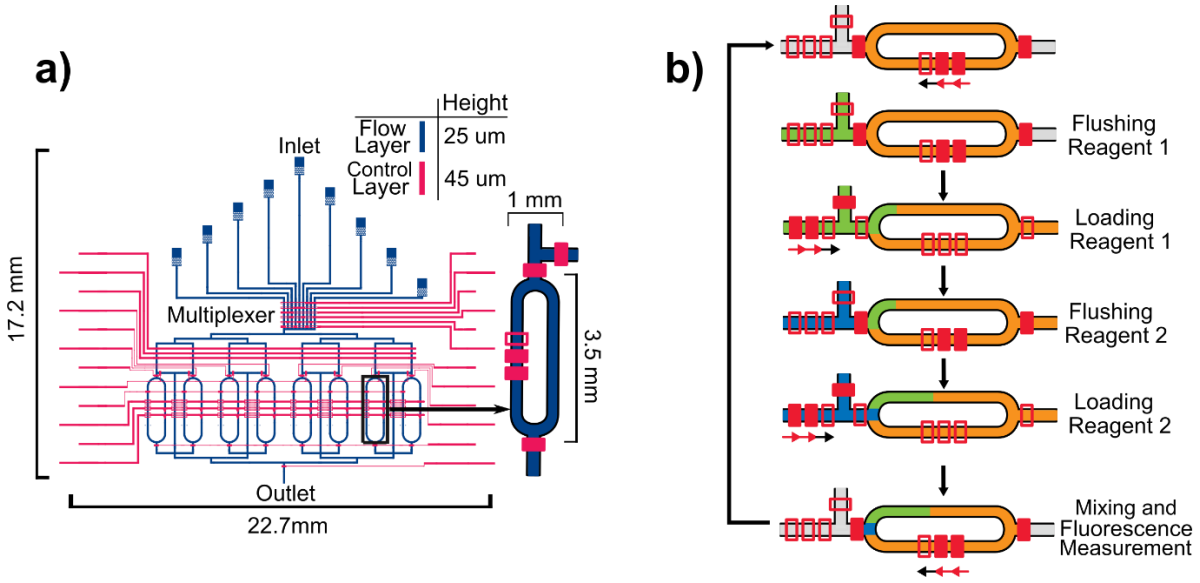

Figure S18(a) Top-view schematic of the pneumatically actuated bi-layer µCSTR microfluidic device used to conduct steady-state TX-TL experiments. The microfluidic devices comprise eight unique 11 nL reactors. The control layer (magenta) regulates the flow of fluids within the flow layer (blue) of the microfluidic device. Reaction solutions are injected into the device via the inlets under constant pressure, with the control channels regulating the flow speed and direction within the device. **(b)** Schematic of the flushing, loading and mixing of reagents inside a reactor. The regions where the control channels intersect the flow channels is indicated with red rectangles (filled rectangles – control channel is pressurized thus inhibiting flow, and unfilled rectangles – control channel is depressurized, thus allowing fluids to flow within the flow channel). One cycle takes approximately 15 mins. (Adapted from Niederholtmeyer *et al*[10])

Molds for the control and flow layers were fabricated using standard photolithography techniques to produce channels with heights of 25 µm and 45 µm respectively. Although the device design being based on previously reported microfluidic devices by Niederholtmeyer *et al.*[10], our research makes use of a flow layer with a uniform feature height, as opposed to the use of multiple channel heights within the same layer of the microfluidic device. The final microfluidic chips were fabricated from PDMS using standard soft lithography methods[11].

Within the microfluidic device, the top layer (flow layer) houses the TX-TL reactions, whilst the water-filled bottom layer (control layer) regulates the flow of fluids in the flow layer (Figure S18a). Each microfluidic device contains eight independent, 11 nL ring reactors, allowing the simultaneously conduction of eight unique reactions. Reaction reagents are injected into the flow layer device using constant pressure via nine inlets. To regulate the flow, each of the 23 control channels located within the control layer of the microfluidic device can be actuated; a process wherein the fluid within the control channel is pressurized causing the control channel to expand. Of the nine possible inflow reagents, only one solution is permitted to flow into the remainder of the microfluidic device at any one time, a process achieved by the incorporation of a multiplexer – a series of control channels operating in conjunction with each other to inhibit all but one inflow solution at any one point in time. Furthermore, each of the eight ring reactors is presided over by a uniquely addressable inlet and outlet control channel – the opening and closing of which enables the periodic injection of reagents into the reactors over the course of an experiment.

Over the course of any TX-TL experiment, three distinct fluid operations are repeatedly called upon (Figure S18b). Firstly, any reagent that needs to be added to the reaction solution currently residing in the reactor is flown into the device. This process is referred to as flushing since any residual reagents present in the flow channel are *flushed* out of the device. During the flushing process the inlets of the reactors remain closed. Subsequently, the desired reagent is loaded into the reactors, simultaneously displacing an equal volume of the reaction products from the reactor. For each of the reaction reagents, the flushing and loading protocols are repeated. Finally, all the reagents in the reactors are mixed and fluorescence signal is measured. This cycle takes approximately 15 mins and is repeated for 10 hours. The cycle time can be reduced or increased by altering the duration of mixing.

The periodicity of injections into the reactors, combined with the volume fraction of the reactor displaced during each injection, is represented by the **Refresh Rate** (min^{-1}) [Table S3]. By changing the **Refresh Rate**, it is possible to control the kinetics of the TX-TL reactions inside the reactors (Figure S19). Our homemade TX-TL system was stable for 10 hours after which the efficiency of the reaction gradually decreases.

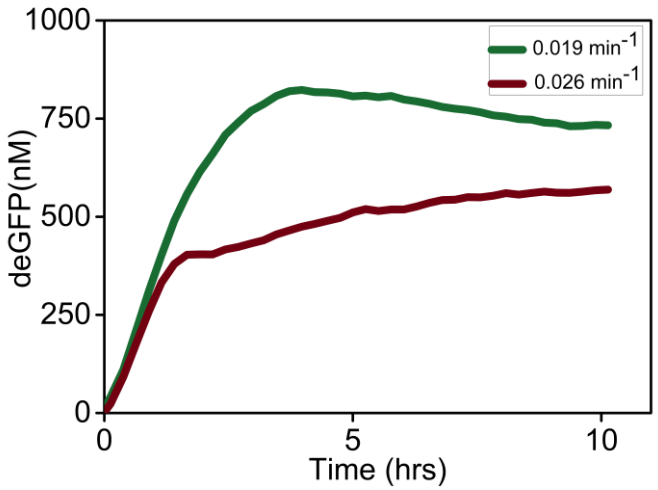

Figure S19 Steady state experiment with 8 nM of **P_{70}-deGFP** template and 1 nM of **P_{70}-σ_{28}** template. Upon changing the Refresh Rate from 0.019 min^{-1} to 0.026 min^{-1} the system adopts a lower steady-state.

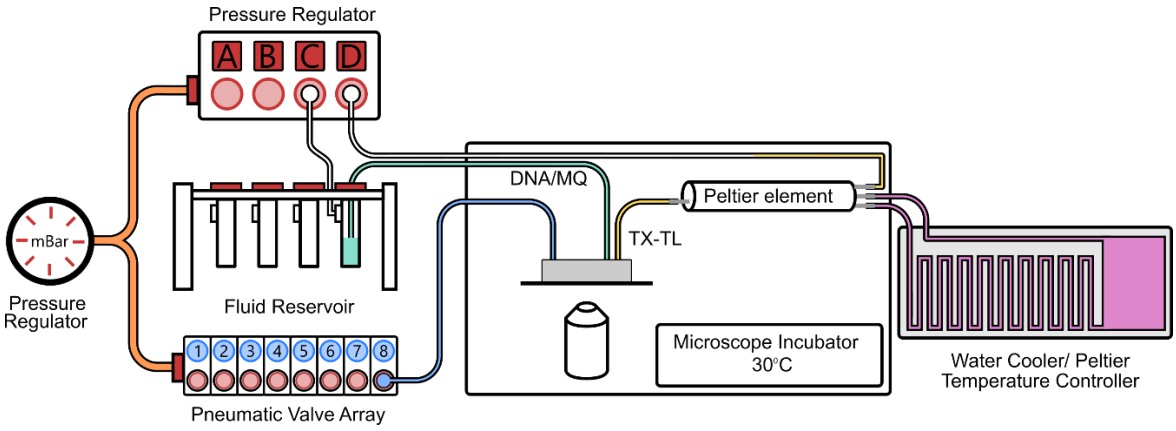

Figure S20 Schematic of the microfluidic set-up. The microfluidic chip is placed above an inverted microscope within an incubator. The TX-TL mix is injected via a Peltier element cooled at 4 ˚C and DNA templates and MQ are kept at 30 ˚C and injected using constant pressure.

During an experiment, the microfluidic chip was placed within a temperature-controlled incubation chamber above an inverted microscope which allowed for the fluorescence imaging of the reactors at a constant temperature (30 ˚C). The TX-TL reaction mixture was loaded into a Peltier device which was maintained at 4 ˚C using a water-based cooling system. The Peltier device was mounted within the incubator as close as possible to the microfluidic device, minimizing the transfer distance of the TX-TL reaction solution upon exiting cooling unit and entering the microfluidic device. DNA templates and MQ water were stored in Tygon tubing (0.02" ID, 0.06" OD) which was placed within the incubator. The injection of all reaction solutions – cooled and uncooled – into the microfluidic device was achieved using constant pressure supplied by a digital pressure control system (Fluigent, MFCS-EZ) (Figure S20).

Experimental Procedure

Calibration

Prior to use, each microfluidic chip requires a calibration to be performed to account for device-specific variations which originate during the fabrication (Figure S21a). When injecting the inflow solutions into the microfluidic device, control channels are utilized in a peristaltic manner to pump the fluid into the remainder of the microfluidic device in a controlled and quantifiable manner. During the calibration procedure, the volume fraction of the ring reactors displaced during a single peristaltic pump cycle can be determined for each of the reactors. Following the calibration, the calculated refresh fraction of each reactor (i.e. the volume fraction displaced in each reactor during a single peristaltic pump cycle) is used to achieve the desired reaction composition. In this manner, a specific volume fraction of the reactor can be displaced in a reliable fashion (Figure S21b).

On-chip Batch TX-TL reactions (Figure S21c)

1. Flush device with TX-TL reaction mixture
2. Load reactors fully with TX-TL reaction mixture.
3. Flush device with **P_{70}-deGFP** template.
4. Load 20% of reactor volume with **P_{70}-deGFP** template.
5. Mix continuously for 30 minutes whilst measuring fluorescence every two minutes.

Steady-state TX-TL reaction

0. Initial Filling of the Device:
   (i) Flush device with TX-TL reaction mixture. Fully load the reactors with TX-TL reaction mixture.
   (ii) Flush device with MQ H_2O.
   (iii) Displace desired volume (corresponding to the Refresh Rate) of the reactor volume with MQ H_2O.
   (iv) Mix (Number of mix cycles determined by setting in Labview Software. Normally 3).

Repeated Cycle:

1. Image each reactor with fluorescence microscope.
2. Flush device with TX-TL mix and pump desired volume into each reactor.
3. Flush device with DNA templates and load the desired volume into each reactor. If more than one DNA solution is being used, the individual solutions are flushed and loaded sequentially.
4. Flush device with MQ H_2O and load desired volume into each reactor.
5. Mix contents of each reactor until a period of approximately 15 minutes has elapsed since the previous image was taken.
6. Repeat from Step 1.

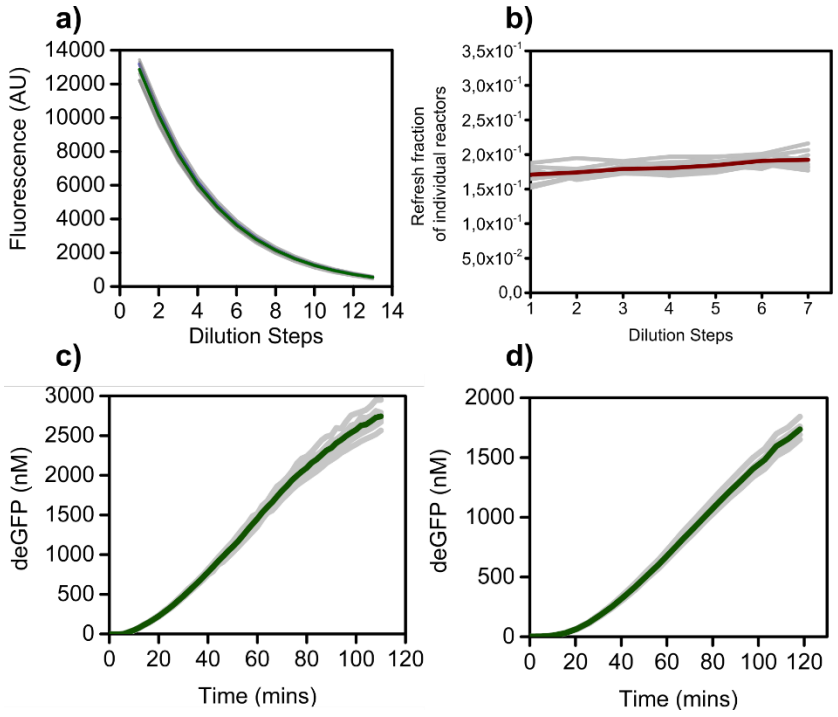

Figure S21 (a) Calibration of microfluidic device prior to a TX-TL experiment. During the calibration procedure, the microfluidic devices are filled with a FITC-Dextran solution, which is subjected to multiple dilution steps. The decrease in fluorescence intensity can subsequently be correlated to the volume fraction of the reactor displaced during each dilution cycle. Since each dilution cycle is performed by executing a set number of peristaltic pumps, it is therefore also possible to determine the number of pump cycles required to displace a desired volume fraction during later experiments. The green line is the average of eight reactors (gray). **(b)** The refresh fraction of individual reactors calculated from (a). The grey lines indicate the individual refresh fractions of each reactor. The red line is the average of the eight reactors (gray). **(c)**The deGFP fluorescence intensity of each of the microfluidic reactors over time during the execution of an on-chip batch experiment. TX-TL mix and 2 nM **P_{70}-deGFP** template are loaded into individual reactors and mixed continuously for 120 mins. Fluorescence is recorded every two minutes. The grey lines indicate the individual fluorescence traces of each reactor. The green line is the average of the eight reactors**. (d)** Batch kinetics for 2 nM **P_{70}-deGFP** template conducted in TECAN plate reader. The green line is the average of four individual measurements (gray).

Parameters	LHS & Fit Boundaries	Batch	Flow
kf_RS28 (nM min^{-1})	0.01-100	2.83	0.55
kf_RS70 (nM min^{-1})	0.01-100	0.085	0.88
kr_RS28 (nM min^{-1})	0.01-100	2.42	0.012
Kr_RS70 (nM min^{-1})	0.01-100	1.668	2.89
kd_s28(nM)	0.1-500	3.58	208
kd_S70 (nM)	0.1-500	4.308	18.89
kd_ci (nM)	0.1-500	28.13*	1.12
vmax_s70 (nM min^{-1})	0.4-3.5	0.99	N/A
vmax_s28 (nM min^{-1})	0.4-3.5	0.53	0.77
vmax_s70ci (nM min^{-1})	0.4-3.5	0.69	3.5
k_trans_ci (nM min^{-1})	0.3-3.5	1.88	0.72
k_trans_GFP(nM min^{-1})	0.3-3.5	0.43	0.771
k_trans_s28 (nM min^{-1})	0.3-3.5	1.70	0.60
N70	1-4.	1	1
N28	1-12.	1.87	1.95
Nci	1-12.	3.12	5.24
deg_mRNA (min^{-1})	0.06-0.2	0.063	0.16
deg_s70 (min^{-1})	0.005-0.01	0.0053	0.0088
deg_GFP (min^{-1})	0.005-0.01	0.0076	0.0061
deg_ci (min^{-1})	0.01-0.02	0.053	0.023
RNAP_0 (nM min^{-1})	50-200	146.97	94.8
S70_0 (nM min^{-1})	35-200	78.66	139.88
k_mat (min^{-1})	N/A	0.044	0.044

Table S1 Parameter table, the first column shows the parameter ID, the second column the boundaries that were maintained for the LHS analysis and the parameter estimation. The third column shows the parameters of the initial estimation using batch data, these parameter were used to characterize the control space of the σ_{28}-

oscillator. The fourth column shows the re-estimation of these parameters using data from the steady-state TX-TL experiments (best fit). Note that the strength and speed of the activation of the feedback loop is overestimated in the initial fit, the forward rate of σ_{28} is lowered and the $Kd's$ for the activation are increased after re-estimating the parameters. We cannot claim that these parameters are as if measured individually. However, we can claim that the parameter set obtained from flow TX-TL can predict the behavior of our network quantitatively – local to the fit – and qualitatively as we move our control points. The $vmax_{RS70}$ parameter only appears in the modified network in the transcriptional activation by σ_{28} batch TX-TL experiment, the maturation rate of deGFP was taken from Niederholtmeyer *et al*[6].

a)

Parameter	Mean fitted value	Standard deviation
'Kr_RS70' (nM min^{-1}) :	16.159589191964137	27.99867962636388)
'N28':	4.075223899722465	2.9348375995794593
'N70':	2.220193180621786	0.979954159342429
'Nci':	5.448686855022009	2.973762310074054
'RNAP0'(nM min^{-1}):	109.87865072318995	40.74506000792622
'S70_0'(nM min^{-1}):	95.72419098850507	44.40075753508003
'deg_GFP'(min^{-1}):	0.006101409700261121	0.0010058072168970082
'deg_ci'(min^{-1}):	0.01453356353427963	0.0029280951198938742
'deg_mRNA'(min^{-1}):	0.11235417908131247	0.03359744093667589
'deg_pol'(min^{-1}):	0.006500827074422545	0.0013902215871766659
'deg_s28'(min^{-1}):	0.00676643919563541	0.0011002968244424175
'deg_s70'(min^{-1}):	0.006534424861005492	0.0010714332616211723
'k_trans_GFP' (nM min^{-1}):	0.6664782915920631	0.2510666725359079
'k_trans_ci' (nM min^{-1}):	1.2989398727956052	0.8621581762857072
'k_trans_s28' (nM min^{-1}):	1.2937410070642381	0.8674933317928915
'kd_ci'(nM):	56.476018800971275	116.37218953720176
'kd_s28'(nM):	57.354702503814764	115.86166513430874
'kd_s70'(nM):	9.99949667167705	14.384453343029387
'kf_RS28' (nM min^{-1}):	11.06352905839121	20.797424291927292
'kf_RS70' (nM min^{-1}):	7.422460242541421	17.438432964177
'kr_RS28' (nM min^{-1}):	16.026324247311308	26.928668433343162
'vmax_s28' (nM min^{-1}):	1.4945300741761587	0.8421960778109105
'vmax_s70ci' (nM min^{-1}):	0.8454753820001012	0.4049560369932143

b)

Parameter	Mean fitted value	Standard deviation
'Kr_RS70' (nM min^{-1}):	12.322676350350124	25.861140341914485
'N28':	4.624601627523838	3.487418896587355
'N70':	2.0126939674770283	0.7735194041299848
'RNAP0'(nM min^{-1}):	105.1833912197974	44.27188675589488
'S70_0'(nM min^{-1}):	96.76233792495583	42.38104083421473
'deg_GFP'(min^{-1}):	0.00610003071668642	0.0009229857396688465
'deg_mRNA'(min^{-1}):	0.12287951859627619	0.0374047399981391
'deg_pol'(min^{-1}):	0.006392671758733013	0.0011892084854877734
'deg_s28'(min^{-1}):	0.006714787723921 3975	0.001220386418024155
'deg_s70'(min^{-1}):	0.0070178554264953	0.0011755487392045056
'k_trans_GFP' (nM min^{-1}):	0.9000275624714896	0.5309323606220361

'k_trans_s28'(nM min^{-1}):	1.0048768824560244	0.7807212071821952
'kd_s28'(nM):	16.13343743909459	33.23749729391245
'kd_s70'(nM):	96.87409974167227	135.9207083621812
'kf_RS28'(nM min^{-1}):	6.234995493937072	15.260724729268413
'kf_RS70'(nM min^{-1}):	13.501850411517017	21.504753596876903
'kr_RS28'(nM min^{-1}):	17.678302000541198	27.547566254401325
'vmax_s28'(nM min^{-1}):	1.2050016552927492	0.5984443605945438
'vmax_s70'(nM min^{-1}):	1.0975789380154135	0.7458679084206213

(c)

Parameter	Mean fitted value	Standard deviation
'Kr_RS70'(nM min^{-1}):	9.517681459025791	20.633509062075436
'N28':	4.409894721274602	3.004416021390059
'N70':	1.3255896103366986	0.410604230581895
'Nci':	5.674307043848433	2.5006618717935565
'RNAP0'(nM min^{-1}):	102.98500523754161	39.147547307230845
'S70_0'(nM min^{-1}):	94.31280058141019	46.400651965756765
'deg_GFP'(min^{-1}):	0.00554091651398632	0.0007649900621338461
'deg_ci'(min^{-1}):	0.015035707366634888	0.0028231281211403433
'deg_mRNA'(min^{-1}):	0.10257449514447275	0.03971279016125567
'deg_pol'(min^{-1}):	0.006302997327800378	0.0012850805135376782
'deg_s28'(min^{-1}):	0.00724195800960205	0.0010944374330752356
'deg_s70'(min^{-1}):	0.006358010868153345	0.001146224308594778
'k_trans_GFP'(nM min^{-1}):	0.5370698831668395	0.1809804487486548
'k_trans_ci'(nM min^{-1}):	1.4107566341384543	0.8116427407461737
'k_trans_s28'(nM min^{-1}):	1.5930921455643403	1.0333372395139389
'kd_ci':	27.242376823945893	70.32317094797294
'kd_s28'(nM):	51.09831845393592	105.21719309051461
'kd_s70'(nM):	25.724341151910004	57.75039162746223
'kf_RS28'(nM min^{-1}):	11.938744960219179	23.766691648047235
'kf_RS70'(nM min^{-1}):	7.993140613946966	15.139909736928987
'kr_RS28'(nM min^{-1}):	6.121044697166394	14.859535934440624
'vmax_s28'(nM min^{-1}):	1.7211259931911855	1.0102601227493149
'vmax_s70ci'(nM min^{-1}):	0.960272185884429	0.3864388425649673

(d)

Parameter	Mean fitted value	Standard deviation
'Kr_RS70'(nM min^{-1}):	2.622603401985375	2.321736774604341
'Nci':	2.1111400137786434	0.2937653250125291
'deg_GFP'(min^{-1}):	0.005525517580944312	0.0006516970785184448
'deg_ci'(min^{-1}):	0.012931142724098368	0.00270272663806615
'deg_mRNA'(min^{-1}):	0.11601004460580172	0.04510583718321941
'deg_pol'(min^{-1}):	0.00659855987665581	0.001083083821561135
'deg_s28'(min^{-1}):	0.006600945225736989	0.001030439681170943
'deg_s70'(min^{-1}):	0.006771141103587754	0.0012577917186110726
'k_trans_GFP'(nM min^{-1}):	0.6407719005741392	0.2914631833972964
'k_trans_ci'(nM min^{-1}):	0.7177874145905991	0.45199888827789253)
'k_trans_s28'(nM min^{-1}):	0.9191184351636297	0.48788514557581064
'kd_ci'(nM):	31.453350680776143	23.541203605172317
'kd_s28'(nM):	47.47144935212406	30.017596313141205
'kd_s70'(nM):	1.4155098121627652	5.513282926988654

'kf_RS28'(nM min^{-1}):	5.376082717418675	3.682587486332795
'kf_RS70'(nM min^{-1}):	0.9926321013048001	0.9695141191641089
'kr_RS28'(nM min^{-1}):	0.617673483339139	1.0257139593242308
'vmax_s28'(nM min^{-1}):	1.1137264114200196	0.6986634398398133
'vmax_s70ci'(nM min^{-1}):	0.762478440565949	0.34324717044536024

(e)

Parameter	Mean fitted value	Standard deviation
'Kr_RS70'(nM min^{-1}):	18.04865788543049	27.902227521657625
'N28':	4.590928076290106	3.4538097597635624
'N70':	2.1705783855386382	0.8396097719059497
'Nci':	6.237411268824316	3.0170670680837404
'RNAP0'(nM min^{-1}):	102.01416127200943	45.382166321922774
'S70_0'(nM min^{-1}):	102.96885141180141	50.59086623387145
'deg_GFP'(min^{-1}):	0.0063985057220058775	0.0012124346603059179
'deg_ci'(min^{-1}):	0.01619953637497264	0.0035933803114041973
'deg_mRNA'(min^{-1}):	0.13755315596266604	0.04146186497902672
'deg_pol'(min^{-1}):	0.007436208442156369	0.0014057854594031133
'deg_s28'(min^{-1}):	0.007436075854440483	0.001584744124343749
'deg_s70'(min^{-1}):	0.007087693423199525	0.001543066906356675
'k_trans_GFP'(nM min^{-1}):	1.3539956895483276	0.9108258883380903
'k_trans_ci'(nM min^{-1}):	1.1462038014951137	0.814929682778412
'k_trans_s28'(nM min^{-1}):	1.2248534802121493	0.8450653885403728
'kd_ci'(nM):	84.82423639458115	135.39002788879262
'kd_s28'(nM):	72.72964714598696	122.12457583482947
'kd_s70'(nM):	51.873795888713744	101.31166323022761
'kf_RS28'(nM min^{-1}):	25.737056280087614	39.27748277189572
'kf_RS70'(nM min^{-1}):	13.287255725596252	28.411011536617753
'kr_RS28'(nM min^{-1}):	13.716408287379078	25.290794744420992
'vmax_s28'(nM min^{-1}):	1.3668336107492285	0.9083907135137076
'vmax_s70ci'(nM min^{-1}):	1.8170990960843822	1.0984248380910067

Table S2 Mean fitted value and Standard deviation for each parameter value for each data set :- **(a)** Single protein expression **(b)** σ_{28}-activation cascade **(c)** Competition between σ_{28} and σ_{70} for core RNAP **(d)** Repression by C1 and **(e)** Steady-state TX-TL data. From the batch data we take the corresponding subset of relevant paramters (for ex. From dataset (b) the σ_{28}-cascade we obtain parameters relevant to σ_{28}-RNAP binding and σ_{28}-transcription).

Reactor volume replaced per 15 mins (%)	**Volume fraction replaced per 15 mins**	**Refresh Rate (min^{-1})**
20	0.2	0.013
30	0.3	0.0195

40	0.4	0.026

Table S3 Refresh ratio calculations for various displacement volumes.

NOTE ON VARIABILITY

Each facet of this work – TX-TL mixture, microfluidic set-up and the mathematical modelling – contributes to certain degree of variability. The primary source of variability arises from the batch-to-batch differences in the TX-TL mixtures. The rates of individual reactions, protein yields have been known to vary across different batches of TX-TL mixtures[9]. Since these contribute to determining network behaviour, all analysis is valid for a given batch of TX-TL mix. Secondly, experimental conditions in a microfluidic chip during a run were carried out in duplicates i.e. two independent reactors in the same chip with the same DNA template concentrations and **Refresh Rate**. Under such conditions we observed negligible variation among oscillations occurring across different reactors (Figure S13a). We observed a marginal variation in oscillation amplitude (approximately 20 nM) upon repeating an experiment across three microfluidic chips (Figure S13b). Hence, we grouped our model predictions into intervals of at least 20 nM to account for such variability (Figures 3b and 4a).

Next, the nature of the model and the reliance on a single output (deGFP) makes parameter estimation a challenging endeavour. First the model lacks mechanistic detail, therefore, processes not captured by the model cause estimated rates to be a function of the control parameters (e.g. competition for resources as DNA concentrations increase) potentially biasing the system to specific experimental conditions (therefore we always estimate rates using more than one condition simultaneously). Second the lack of additional observable states means we obtain a distribution of parameter sets equally capable of describing the data. We sought to mitigate this effect by setting boundaries on each parameter, doing a global

sensitivity analysis between the boundaries to scope out qualitative differences in behavior, estimating specific rates of the network from targeted batch TX-TL experiments and finally by fitting to steady-state TX-TL experiments. Overall, this means that there is no single parameter set which can describe all the experiments but rather a distribution (Figures S7 a,b and c, S14 a and b , S15 a and b), which showed qualitative agreement (with one another and the global sensitivity analysis) but quantitative differences (e.g. Figures S5 and S7). From this we chose the best set (Figure S7 d and e, Table S1) to present the oscillating subset of the control parameter space (Figure S8a and S11a) and the local sensitivity analysis (Figure S9 and S10). Hence, our theoretical approach captures trends of network behavior local to the fit and is able to qualitatively guide network modifications.

DNA Sequences

Promoter Gene Sequence ssra tag

(Note: All promoters here denote the 'a' variant as mentioned in Garamella *et al*[12]. For example, P_{70} denotes P_{70a}).

DNA name	Sequence
P_{70}-deGFP	ATAGGGGTTCCGCGCACATTTCCCCGAAAAGTGCCACC TGACGTCTAAGAAACCATTATTATCATGACATTAACCT ATAAAAATAGGCGTATCACGAGGCCCTTTCGTCTTCAA GAATTCTGGCGAATCCTCTGACCAGCCAGAAAACGACC TTTCTGTGGTGAAACCGGATGCTGCAATTCAGAGCGCC AGCAAGTGGGGGACAGCAGAAGACCTGACCGCCGCAG AGTGGATGTTTGACATGGTGAAGACTATCGCACCATCA GCCAGAAAACCGAATTTTGCTGGGTGGGCTAACGATAT CCGCCTGATGCGTGAACGTGACGGACGTAACCACCGCG ACATGTGTGTGCTGTTCCGCTGGGCATGCTGAGCTAAC ACCGTGCGTGTTGACAATTTTACCTCTGGCGGTGATAAT GGTTGCAGCTAGCAATAATTTTGTTTAACTTTAAGAAG GAGATATACCATGGAGCTTTTCACTGGCGTTGTTCCCAT CCTGGTCGAGCTGGACGGCGACGTAAACGGCCACAAGT TCAGCGTGTCCGGCGAGGGCGAGGGCGATGCCACCTAC GGCAAGCTGACCCTGAAGTTCATCTGCACCACCGGCAA GCTGCCCGTGCCCTGGCCCACCCTCGTGACCACCCTGA CCTACGGCGTGCAGTGCTTCAGCCGCTACCCCGACCAC ATGAAGCAGCACGACTTCTTCAAGTCCGCCATGCCCGA AGGCTACGTCCAGGAGCGCACCATCTTCTTCAAGGACG ACGGCAACTACAAGACCCGCGCCGAGGTGAAGTTCGA GGGCGACACCCTGGTGAACCGCATCGAGCTGAAGGGC

	ATCGACTTCAAGGAGGACGGCAACATCCTGGGGCACA AGCTGGAGTACAACTACAACAGCCACAACGTCTATATC ATGGCCGACAAGCAGAAGAACGGCATCAAGGTGAACT TCAAGATCCGCCACAACATCGAGGACGGCAGCGTGCA GCTCGCCGACCACTACCAGCAGAACACCCCCATCGGCG ACGGCCCCGTGCTGCTGCCCGACAACCACTACCTGAGC ACCCAGTCCGCCCTGAGCAAAGACCCCAACGAGAAGC GCGATCACATGGTCCTGCTGGAGTTCGTGACCGCCGCC GGGATCTAACTCGAGCAAAGCCCGCCGAAAGGCGGGC TTTTCTGTGTCGACCGATGCCCTTGAGAGCCTTCAACCC AGTCAGCTCCTTCCGGTGGGCGCGGGGCATGACTATCG TCGCCGCACTTATGACTGTCTTCTTTATCATGCAACTCG TAGGACAGGTGCCGGCAGCGCTCTTCCGCTTCCTCGCT CACTGACTCGCTGCGCTCGGTCGTTCGGCTGCGGCGAG CGGTATCAGCTCACTCAAAGGCGGTAATACGGTTATCC ACAGAATCAGGGGATAACGCAGGAAAGAACATGTGAG CAAAAGGCCAGCAAAAGGCCAGGAACCGTAAAAAGGC CGCGTTGCTGGCGTTTTTCCATAGGCTCCGCCCC
P_{70}-σ_{28}	CGAGGCCCTTTCGTCTTCAAGAATTCTGGCGAATCCTCT GACCAGCCAGAAAACGACCTTTCTGTGGTGAAACCGGA TGCTGCAATTCAGAGCGCCAGCAAGTGGGGGACAGCA GAAGACCTGACCGCCGCAGAGTGGATGTTTGACATGGT GAAGACTATCGCACCATCAGCCAGAAAACCGAATTTTG CTGGGTGGGCTAACGATATCCGCCTGATGCGTGAACGT GACGGACGTAACCACCGCGACATGTGTGTGCTGTTCCG CTGGGCATGCCAGGACAACTTCTGGTCCGGTAACGTGC TGAGCTAACACCGTGCGTGTTGACAATTTTACCTCTGGC GGTGATAATGGTTGCAGCTAGCAATAATTTTGTTTAACT TTAAGAAGGAGGATCCAAATGAATTCACTCTATACCGC TGAAGGTGTAATGGATAAACACTCGCTGTGGCAGCGTT ATGTCCCGCTGGTGCGTCACGAAGCATTGCGCCTGCAG GTTCGACTGCCCGCGAGCGTGGAACTTGACGATCTGCT ACAGGCGGGCGGCATTGGGTTACTTAATGCCGTCGAAC GCTATGACGCCCTACAAGGAACGGCATTTACAACTTAC GCAGTGCAGCGTATCCGTGGCGCTATGCTGGATGAACT TCGCAGCCGTGACTGGGTGCCGCGCAGCGTGCGACGCA ACGCGCGTGAAGTGGCACAGGCAATAGGGCAACTGGA GCAGGAACTTGGCCGCAACGCCACGGAAACTGAGGTA GCGGAACGTTTAGGGATCGATATTGCCGATTATCGCCA AATGTTGCTCGACACCAATAACAGCCAGCTCTTCTCCT ACGATGAGTGGCGCGAAGAGCACGGCGATAGCATCGA ACTGGTTACTGATGATCATCAGCGAGAAAACCCGCTAC AACAACTACTGGACAGTAATCTGCGCCAGCGGGTGATG GAAGCCATCGAAACGTTGCCGGAGCGCGAAAAACTGG TATTAACCCTCTATTACCAGGAAGAGCTGAATCTCAAA GAGATTGGCGCGGTGCTGGAGGTCGGGGAATCGCGGG TCAGTCAGTTACACAGCCAGGCTATTAAACGGTTACGC ACTAAACTGGGTAAGTTATAATCTAGAGGCGCCACTCG AGAGTCGACCAAAGCCCGCCGAAAGGCGGGCTTTTCTG TGCCGGCATGATAAGCTGTCAAACATGAGAATTGCAAC TTATATCGTATGGGGCTGACTTCAGGTGCTACATTTGAA GAGATAAATTGCACTGAAATCTAGAAATATTTTATCTG ATTAATAAGATGATCTTCTTGAGATCGTTTTGGTCTGCG CGTAATCTCTTGCTCTGAAAACGAAAAAACCGCCTTGC AGGGCGGTTTTTCGAAGGTTCTCTGAGCTACCAACTCTT T
P_{28}-C1-ssra	ATAGGGGTTCCGCGCACATTTCCCCGAAAAGTGCCACC

	TGACGTCTAAGAAACCATTATTATCATGACATTAACCT ATAAAAATAGGCGTATCACGAGGCCCTTTCGTCTTCAA GAATTCTGGCGAATCCTCTGACCAGCCAGAAAACGACC TTTCTGTGGTGAAACCGGATGCTGCAATTCAGAGCGCC AGCAAGTGGGGGACAGCAGAAGACCTGACCGCCGCAG AGTGGATGTTTGACATGGTGAAGACTATCGCACCATCA GCCAGAAAACCGAATTTTGCTGGGTGGGCTAACGATAT CCGCCTGATGCGTGAACGTGACGGACGTAACCACCGCG ACATGTGTGTGCTGTTCCGCTGGGCATGCCAGGACAAC TTCTGGTCCGGTAACGTGCTGAGCCCGGCCAAGCTTCA ATAAAGTTTCCCCCCTCCTTGCCGATAACGAGATCAAG CTAGCAATAATTTTGTTTAACTTTAAGAAGGAGATATA CATATGAGCACAAAAAAGAAACCATTAACACAAGAGC AGCTTGAGGACGCACGTCGCCTTAAAGCAATTTATGAA AAAAAGAAAAATGAACTTGGCTTATCCCAGGAATCTGT CGCAGACAAGATGGGGATGGGGCAGTCAGGCGTTGGT GCTTTATTTAATGGCATCAATGCATTAAATGCTTATAAC GCCGCATTGCTTGCAAAAATTCTCAAAGTTAGCGTTGA AGAATTTAGCCCTTCAATCGCCAGAGAAATCTACGAGA TGTATGAAGCGGTTAGTATGCAGCCGTCACTTAGAAGT GAGTATGAGTACCCTGTTTTTTCTCATGTTCAGGCAGGG ATGTTCTCACCTGAGCTTAGAACCTTTACCAAAGGTGA TGCGGAGAGATGGGTAAGCACAACCAAAAAAGCCAGT GATTCTGCATTCTGGCTTGAGGTTGAAGGTAATTCCATG ACCGCACCAACAGGCTCCAAGCCAAGCTTTCCTGACGG AATGTTAATTCTCGTTGACCCTGAGCAGGCTGTTGAGC CAGGTGATTTCTGCATAGCCAGACTTGGGGGTGATGAG TTTACCTTCAAGAAACTGATCAGGGATAGCGGTCAGGT GTTTTTACAACCACTAAACCCACAGTACCCAATGATCC CATGCAATGAGAGTTGTTCCGTTGTGGGGAAAGTTATC GCTAGTCAGTGGCCTGAAGAGACGTTTGGCTGTGCAGC AAACGACGAAAACTACGCTTTAGCTGCTTAAGAGCTCC GTCGACAAGCTTGCGGCCGCACTCGAGCAAAGCCCGCC GAAAGGCGGGCTTTTCTGTGTCGACCGATGCCCTTGAG AGCCTTCAACCCAGTCAGCTCCTTCCGGTGGGCGCGGG GCATGACTATCGTCGCCGCACTTATGACTGTCTTCTTTA TCATGCAACTCGTAGGACAGGTGCCGGCAGCGCTCTTC CGCTTCCTCGCTCACTGACTCGCTGCGCTCGGTCGTTCG GCTGCGGCGAGCGGTATCAGCTCACTCAAAGGCGGTAA TACGGTTATCCACAGAATCAGGGGATAACGCAGGAAA GAACATGTGAGCAAAAGGCCAGCAAAAGGCCAGGAAC CGTAAAAAGGCCGCGTTGCTGGCGTTTTTCCATAGGCT CCGCCCC
P_{70}-σ_{19}	CGAGGCCCTTTCGTCTTCAAGAATTCTGGCGAATCCTCT GACCAGCCAGAAAACGACCTTTCTGTGGTGAAACCGGA TGCTGCAATTCAGAGCGCCAGCAAGTGGGGGACAGCA GAAGACCTGACCGCCGCAGAGTGGATGTTTGACATGGT GAAGACTATCGCACCATCAGCCAGAAAACCGAATTTTG CTGGGTGGGCTAACGATATCCGCCTGATGCGTGAACGT GACGGACGTAACCACCGCGACATGTGTGTGCTGTTCCG CTGGGCATGCCAGGACAACTTCTGGTCCGGTAACGTGC TGAGCTAACACCGTGCGTGTTGACAATTTTACCTCTGGC GGTGATAATGGTTGCAGCTAGCAATAATTTTGTTTAACT TTAAGAAGGAGGATCCAAATGTCTGACCGCGCCACTAC CACAGCTTCCTTAACGTTCGAGTCGCTTTATGGCACACA TCACGGCTGGTTGAAAAGCTGGCTGACGCGCAAACTCC AGTCTGCTTTTGATGCAGATGACATTGCCCAGGACACT TTTTTGCGGGTAATGGTCAGCGAAACGCTCTCGACGAT CCGCGATCCTCGCTCCTTCCTCTGCACTATCGCCAAACG

	CGTGATGGTGGACCTGTTTCGCCGAAACGCGCTGGAAA AAGCGTATCTGGAGATGCTGGCGCTTATGCCGGAGGGG GGAGCGCCTTCACCTGAGGAACGCGAAAGCCAACTCG AGACCCTACAACTCCTCGACAGCATGCTGGACGGGCTA AACGGCAAAACACGTGAAGCGTTTCTGCTTTCGCAACT GGATGGTCTGACATACAGCGAGATTGCGCACAAACTCG GTGTTTCCATCAGCTCCGTGAAAAAATACGTGGCGAAA GCCGTCGAGCACTGCCTGCTGTTCCGTCTGGAGTATGG GTTATGATGTACAAGTAACTCGAGGAATTCCGACTCAA TTAGTTCAGTCAGTTTCAGGATATTAGTCATCTCTACAT TGATTATGAGTATTCAGAAATTCCTTAAATATTCTGACA AATGCTCTTTCCCTAAACTCCCCCCATAAAAAAACCCG CCGAAGCGGGTTTTTACGTTATTTGCGGATTAACGATTA CTCGTTATCAGAACCGCCCAGACCTGCGTTCAGCAGTT CTGCCAGGCTGGCAGATGCGTCTTCCGGAATTGATCCG TCGACCAAAGCCCGCCGAAAGGCGGGCTTTTCTGTGCC GGCATGATAAGCTGTCAAACATGAGAATTGCAACTTAT ATCGTATGGGGCTGACTTCAGGTGCTACATTTGAAGAG ATAAATTGCACTGAAATCTAGAAATATTTTATCTGATTA ATAAGATGATCTTCTTGAGATCGTTTTGGTCTGCGCGTA ATCTCTTGCTCTGAAAACGAAAAAACCGCCTTGCAGGG CGGTTTTTCGAAGGTTCTCTGAGCTACCAACTCTTT
P_{19}-C1-ssra	CGAGGCCCTTTCGTCTTCAAGAATTCTGGCGAATCCTCT GACCAGCCAGAAAACGACCTTTCTGTGGTGAAACCGGA TGCTGCAATTCAGAGCGCCAGCAAGTGGGGGACAGCA GAAGACCTGACCGCCGCAGAGTGGATGTTTGACATGGT GAAGACTATCGCACCATCAGCCAGAAAACCGAATTTTG CTGGGTGGGCTAACGATATCCGCCTGATGCGTGAACGT GACGGACGTAACCACCGCGACATGTGTGTGCTGTTCCG CTGGGCATGCCAGGACAACTTCTGGTCCGGTAACGTGC TGAGCCCGGCCAAGCTTACTGTAAGGAAAATAATTCTT ATTTCGATTGTCCTTTTTACCCTTCTCGTTCGACTCATAG CTGCTAGCAATAATTTTGTTTAACTTTAAGAAGGAGGA TCCAAATGAGCACAAAAAAGAAACCATTAACACAAGA GCAGCTTGAGGACGCACGTCGCCTTAAAGCAATTTATG AAAAAAAGAAAAATGAACTTGGCTTATCCCAGGAATCT GTCGCAGACAAGATGGGGATGGGGCAGTCAGGCGTTG GTGCTTTATTTAATGGCATCAATGCATTAAATGCTTATA ACGCCGCATTGCTTGCAAAAATTCTCAAAGTTAGCGTT GAAGAATTTAGCCCTTCAATCGCCAGAGAAATCTACGA GATGTATGAAGCGGTTAGTATGCAGCCGTCACTTAGAA GTGAGTATGAGTACCCTGTTTTTTCTCATGTTCAGGCAG GGATGTTCTCACCTGAGCTTAGAACCTTTACCAAAGGT GATGCGGAGAGATGGGTAAGCACAACCAAAAAAGCCA GTGATTCTGCATTCTGGCTTGAGGTTGAAGGTAATTCCA TGACCGCACCAACAGGCTCCAAGCCAAGCTTTCCTGAC GGAATGTTAATTCTCGTTGACCCTGAGCAGGCTGTTGA GCCAGGTGATTTCTGCATAGCCAGACTTGGGGGTGATG AGTTTACCTTCAAGAAACTGATCAGGGATAGCGGTCAG GTGTTTTTACAACCACTAAACCCACAGTACCCAATGAT CCCATGCAATGAGAGTTGTTCCGTTGTGGGGAAAGTTA TCGCTAGTCAGTGGCCTGAAGAGACGTTTGGCTGTGCA GCAAACGACGAAAACTACGCTTTAGCTGCTTAATCTAG AGGCGCCACTCGAGAGTCGACCAAAGCCCGCCGAAAG GCGGGCTTTTCTGTGCCGGCATGATAAGCTGTCAAACA TGAGAATTGCAACTTATATCGTATGGGGCTGACTTCAG GTGCTACATTTGAAGAGATAAATTGCACTGAAATCTAG AAATATTTTATCTGATTAATAAGATGATCTTCTTGAGAT CGTTTTGGTCTGCGCGTAATCTCTTGCTCTGAAAACGAA AAAACCGCCTTGCAGGGCGGTTTTTCGAAGGTTCTCTG

	AGCTACCAACTCTTT
P_{70}-deGFP-ssra	ATAGGGGTTCCGCGCACATTTCCCCGAAAAGTGCCACC TGACGTCTAAGAAACCATTATTATCATGACATTAACCT ATAAAAATAGGCGTATCACGAGGCCCTTTCGTCTTCAA GAATTCTGGCGAATCCTCTGACCAGCCAGAAAACGACC TTTCTGTGGTGAAACCGGATGCTGCAATTCAGAGCGCC AGCAAGTGGGGGACAGCAGAAGACCTGACCGCCGCAG AGTGGATGTTTGACATGGTGAAGACTATCGCACCATCA GCCAGAAAACCGAATTTTGCTGGGTGGGCTAACGATAT CCGCCTGATGCGTGAACGTGACGGACGTAACCACCGCG ACATGTGTGTGCTGTTCCGCTGGGCATGCTGAGCTAAC ACCGTGCGTGTTGACAATTTTACCTCTGGCGGTGATAAT GGTTGCAGCTAGCAATAATTTTGTTTAACTTTAAGAAG GAGATATACCATGGAGCTTTTCACTGGCGTTGTTCCCAT CCTGGTCGAGCTGGACGGCGACGTAAACGGCCACAAGT TCAGCGTGTCCGGCGAGGGCGAGGGCGATGCCACCTAC GGCAAGCTGACCCTGAAGTTCATCTGCACCACCGGCAA GCTGCCCGTGCCCTGGCCCACCCTCGTGACCACCCTGA CCTACGGCGTGCAGTGCTTCAGCCGCTACCCCGACCAC ATGAAGCAGCACGACTTCTTCAAGTCCGCCATGCCCGA AGGCTACGTCCAGGAGCGCACCATCTTCTTCAAGGACG ACGGCAACTACAAGACCCGCGCCGAGGTGAAGTTCGA GGGCGACACCCTGGTGAACCGCATCGAGCTGAAGGGC ATCGACTTCAAGGAGGACGGCAACATCCTGGGGCACA AGCTGGAGTACAACTACAACAGCCACAACGTCTATATC ATGGCCGACAAGCAGAAGAACGGCATCAAGGTGAACT TCAAGATCCGCCACAACATCGAGGACGGCAGCGTGCA GCTCGCCGACCACTACCAGCAGAACACCCCCATCGGCG ACGGCCCCGTGCTGCTGCCCGACAACCACTACCTGAGC ACCCAGTCCGCCCTGAGCAAAGACCCCAACGAGAAGC GCGATCACATGGTCCTGCTGGAGTTCGTGACCGCCGCC GGGATCGCAGCAAACGACGAAAACTACGCTTTAGCTGC TTAACTCGAGCAAAGCCCGCCGAAAGGCGGGCTTTTCT GTGTCGACCGATGCCCTTGAGAGCCTTCAACCCAGTCA GCTCCTTCCGGTGGGCGCGGGGCATGACTATCGTCGCC GCACTTATGACTGTCTTCTTTATCATGCAACTCGTAGGA CAGGTGCCGGCAGCGCTCTTCCGCTTCCTCGCTCACTGA CTCGCTGCGCTCGGTCGTTCGGCTGCGGCGAGCGGTAT CAGCTCACTCAAAGGCGGTAATACGGTTATCCACAGAA TCAGGGGATAACGCAGGAAAGAACATGTGAGCAAAAG GCCAGCAAAAGGCCAGGAACCGTAAAAAGGCCGCGTT GCTGGCGTTTTTCCATAGGCTCCGCCCC
P_{28}-deGFP	ATAGGGGTTCCGCGCACATTTCCCCGAAAAGTGCCACC TGACGTCTAAGAAACCATTATTATCATGACATTAACCT ATAAAAATAGGCGTATCACGAGGCCCTTTCGTCTTCAA GAATTCTGGCGAATCCTCTGACCAGCCAGAAAACGACC TTTCTGTGGTGAAACCGGATGCTGCAATTCAGAGCGCC AGCAAGTGGGGGACAGCAGAAGACCTGACCGCCGCAG AGTGGATGTTTGACATGGTGAAGACTATCGCACCATCA GCCAGAAAACCGAATTTTGCTGGGTGGGCTAACGATAT CCGCCTGATGCGTGAACGTGACGGACGTAACCACCGCG ACATGTGTGTGCTGTTCCGCTGGGCATGCCAGGACAAC TTCTGGTCCGGTAACGTGCTGAGCCCGGCCAAGCTTCA ATAAAGTTTCCCCCCTCCTTGCCGATAACGAGATCAAG CTAGCAATAATTTTGTTTAACTTTAAGAAGGAGATATA CCATGGAGCTTTTCACTGGCGTTGTTCCCATCCTGGTCG AGCTGGACGGCGACGTAAACGGCCACAAGTTCAGCGT

	GTCCGGCGAGGGCGAGGGCGATGCCACCTACGGCAAG CTGACCCTGAAGTTCATCTGCACCACCGGCAAGCTGCC CGTGCCCTGGCCCACCCTCGTGACCACCCTGACCTACG GCGTGCAGTGCTTCAGCCGCTACCCCGACCACATGAAG CAGCACGACTTCTTCAAGTCCGCCATGCCCGAAGGCTA CGTCCAGGAGCGCACCATCTTCTTCAAGGACGACGGCA ACTACAAGACCCGCGCCGAGGTGAAGTTCGAGGGCGA CACCCTGGTGAACCGCATCGAGCTGAAGGGCATCGACT TCAAGGAGGACGGCAACATCCTGGGGCACAAGCTGGA GTACAACTACAACAGCCACAACGTCTATATCATGGCCG ACAAGCAGAAGAACGGCATCAAGGTGAACTTCAAGAT CCGCCACAACATCGAGGACGGCAGCGTGCAGCTCGCCG ACCACTACCAGCAGAACACCCCCATCGGCGACGGCCCC GTGCTGCTGCCCGACAACCACTACCTGAGCACCCAGTC CGCCCTGAGCAAAGACCCCAACGAGAAGCGCGATCAC ATGGTCCTGCTGGAGTTCGTGACCGCCGCCGGGATCTA ACTCGAGCAAAGCCCGCCGAAAGGCGGGCTTTTCTGTG TCGACCGATGCCCTTGAGAGCCTTCAACCCAGTCAGCT CCTTCCGGTGGGCGCGGGGCATGACTATCGTCGCCGCA CTTATGACTGTCTTCTTTATCATGCAACTCGTAGGACAG GTGCCGGCAGCGCTCTTCCGCTTCCTCGCTCACTGACTC GCTGCGCTCGGTCGTTCGGCTGCGGCGAGCGGTATCAG CTCACTCAAAGGCGGTAATACGGTTATCCACAGAATCA GGGGATAACGCAGGAAAGAACATGTGAGCAAAAGGCC AGCAAAAGGCCAGGAACCGTAAAAAGGCCGCGTTGCT GGCGTTTTTCCATAGGCTCCGCCCC
P_{19}-deGFP	ATAGGGGTTCCGCGCACATTTCCCCGAAAAGTGCCACC TGACGTCTAAGAAACCATTATTATCATGACATTAACCT ATAAAAATAGGCGTATCACGAGGCCCTTTCGTCTTCAA GAATTCTGGCGAATCCTCTGACCAGCCAGAAAACGACC TTTCTGTGGTGAAACCGGATGCTGCAATTCAGAGCGCC AGCAAGTGGGGGACAGCAGAAGACCTGACCGCCGCAG AGTGGATGTTTGACATGGTGAAGACTATCGCACCATCA GCCAGAAAACCGAATTTTGCTGGGTGGGCTAACGATAT CCGCCTGATGCGTGAACGTGACGGACGTAACCACCGCG ACATGTGTGTGCTGTTCCGCTGGGCATGCCAGGACAAC TTCTGGTCCGGTAACGTGCTGAGCCCGGCCAAGCTTAC TGTAAGGAAAATAATTCTTATTTCGATTGTCCTTTTTAC CCTTCTCGTTCGACTCATAGCTGCTAGCAATAATTTTGT TTAACTTTAAGAAGGAGATATACCATGGAGCTTTTCAC TGGCGTTGTTCCCATCCTGGTCGAGCTGGACGGCGACG TAAACGGCCACAAGTTCAGCGTGTCCGGCGAGGGCGA GGGCGATGCCACCTACGGCAAGCTGACCCTGAAGTTCA TCTGCACCACCGGCAAGCTGCCCGTGCCCTGGCCCACC CTCGTGACCACCCTGACCTACGGCGTGCAGTGCTTCAG CCGCTACCCCGACCACATGAAGCAGCACGACTTCTTCA AGTCCGCCATGCCCGAAGGCTACGTCCAGGAGCGCACC ATCTTCTTCAAGGACGACGGCAACTACAAGACCCGCGC CGAGGTGAAGTTCGAGGGCGACACCCTGGTGAACCGC ATCGAGCTGAAGGGCATCGACTTCAAGGAGGACGGCA ACATCCTGGGGCACAAGCTGGAGTACAACTACAACAGC CACAACGTCTATATCATGGCCGACAAGCAGAAGAACG GCATCAAGGTGAACTTCAAGATCCGCCACAACATCGAG GACGGCAGCGTGCAGCTCGCCGACCACTACCAGCAGA ACACCCCCATCGGCGACGGCCCCGTGCTGCTGCCCGAC AACCACTACCTGAGCACCCAGTCCGCCCTGAGCAAAGA CCCCAACGAGAAGCGCGATCACATGGTCCTGCTGGAGT TCGTGACCGCCGCCGGGATCTAACTCGAGCAAAGCCCG CCGAAAGGCGGGCTTTTCTGTGTCGACCGATGCCCTTG

	AGAGCCTTCAACCCAGTCAGCTCCTTCCGGTGGGCGCG GGGCATGACTATCGTCGCCGCACTTATGACTGTCTTCTT TATCATGCAACTCGTAGGACAGGTGCCGGCAGCGCTCT TCCGCTTCCTCGCTCACTGACTCGCTGCGCTCGGTCGTT CGGCTGCGGCGAGCGGTATCAGCTCACTCAAAGGCGGT AATACGGTTATCCACAGAATCAGGGGATAACGCAGGA AAGAACATGTGAGCAAAAGGCCAGCAAAAGGCCAGGA ACCGTAAAAAGGCCGCGTTGCTGGCGTTTTTCCATAGG CTCCGCCCC

References

(1) Mauri, M., and Klumpp, S. (2014) A Model for Sigma Factor Competition in Bacterial Cells. *PLoS Comput. Biol. 10*, 29–34.

(2) Mangan, S., and Alon, U. (2003) Structure and function of the feed-forward loop network motif. *Proc. Natl. Acad. Sci. U. S. A. 100*, 11980–11985.

(3) Milo, R., Jorgensen, P., Moran, U., Weber, G., and Springer, M. (2009) BioNumbers The database of key numbers in molecular and cell biology. *Nucleic Acids Res. 38*, 750–753.

(4) Novák, B., and Tyson, J. J. (2008) Design principles of biochemical oscillators. *Nat. Rev. Mol. Cell Biol. 9*, 981–91.

(5) Barber, C. B., Dobkin, D. P., and Huhdanpaa, H. (1996) The quickhull algorithm for convex hulls. *ACM Trans. Math. Softw. 22*, 469–483.

(6) Niederholtmeyer, H., Sun, Z. Z., Hori, Y., Yeung, E., Verpoorte, A., Murray, R. M., and Maerkl, S. J. (2015) Rapid cell-free forward engineering of novel genetic ring oscillators. *Elife 4*, 1–18.

(7) Smith, R. W., van Sluijs, B., and Fleck, C. (2017) Designing synthetic networks in silico: A generalised evolutionary algorithm approach. *BMC Syst. Biol. 11*, 1–19.

(8) Helwig, B., van Sluijs, B., Pogodaev, A., Postma, S. and Huck, W. T. S. (2018) Bottom-up Construction of an Adaptive Enzymatic Reaction Network. *Angew. Chemie Int. Ed.* 1–6.

(9) Sun, Z. Z., Hayes, C. a, Shin, J., Caschera, F., Murray, R. M., and Noireaux, V. (2013) Protocols for implementing an Escherichia coli based TX-TL cell-free expression system for synthetic biology. *J. Vis. Exp.* e50762.

(10) Niederholtmeyer, H., Stepanova, V., and Maerkl, S. J. (2013) Implementation of cell-free biological networks at steady state. *Proc. Natl. Acad. Sci. U. S. A. 110*, 15985–90.

(11) Unger, M. A., Unger, M. A., Chou, H., Thorsen, T., Scherer, A., and Quake, S. R. (2013) Monolithic Microfabricated Valves and Pumps by Multilayer Soft Lithography *113*, 113–117.

(12) Garamella, J., Marshall, R., Rustad, M., and Noireaux, V. (2016) The All E. coli TX-TL Toolbox 2.0: A Platform for Cell-Free Synthetic Biology. *ACS Synth. Biol. 5*, 344–355.